

## REPORT No. 705

# WIND-TUNNEL INVESTIGATION OF EFFECT OF INTERFERENCE ON LATERAL-STABILITY CHARACTERISTICS OF FOUR NACA 23012 WINGS, AN ELLIPTICAL AND A CIRCULAR FUSELAGE AND VERTICAL FINS

By RUFUS O. HOUSE and ARTHUR R. WALLACE

### SUMMARY

A wind-tunnel investigation of the effect of wing-fuselage interference on lateral-stability characteristics was made in the NACA 7- by 10-foot wind tunnel. Four NACA 23012 wings were tested in combination with two fuselages and two fins, representing high-wing, low-wing, and midwing monoplanes. The fuselages are of circular and elliptical cross section. The wings have rounded tips and, in plan form, one is rectangular and the other three are tapered 3:1 with various amounts of sweep.

The rate of change in the coefficients of rolling moment, yawing moment, and lateral force with angle of yaw is given in a form to show the increment caused by wing-fuselage interference for the model with no fin and the effect of wing-fuselage interference on fin effectiveness. Results for the fuselage-fin combination and the wing tested alone are also given.

The results showed that wing position had a pronounced effect on lateral-stability characteristics. Wing-fuselage interference increased the effective dihedral in the order of  $5^\circ$  for the high-wing monoplane; a corresponding decrease in effective dihedral was obtained for the low-wing combination. With flaps neutral the maximum interference effect was sufficient to balance as much as 60 percent of the unstable yawing moment of the fuselage. For some cases with the flaps deflected the interference effect was of sufficient magnitude to balance the entire unstable yawing moment of the fuselage. Large changes in fin effectiveness were caused by wing-fuselage interference, the fin effectiveness being decreased about 40 percent for the high-wing monoplane and increased about 80 percent for the low-wing monoplane. Flap deflection increased the fin effectiveness as much as 50 percent.

### INTRODUCTION

Mathematical equations defining the lateral-stability characteristics of airplanes have been available for many years. Charts based on these equations offer a means of rapidly estimating the characteristics of a particular airplane (reference 1). In order to use either the equations or the charts, however, a knowledge of certain basic physical quantities, called stability derivatives, is required. These derivatives are dependent upon a large number of variables and, as a result, progress in their isolation has been slow. Some of the variables affecting the stability derivatives are wing,

fuselage, and fin forms and the aerodynamic interference between these parts.

The stability derivatives are functions of certain aerodynamic factors and of the amount and the distribution of the mass of the airplane. The aerodynamic factors can be divided into three general classifications: those depending on yaw or sideslip, those depending on yawing velocity, and those depending on rolling velocity.

The aerodynamic factors that depend on yaw have been the subject of an extensive investigation by the NACA. The effect on lateral-stability characteristics of various changes in wing variables, such as plan form, taper, sweep, and dihedral is considered in references 2 and 3. A theoretical prediction of some of the lateral-stability characteristics for wings is given in reference 4, and some of the effects of wing-fuselage interference are given in reference 5.

The present investigation is a continuation of the study of the effects of wing-fuselage interference. The wings described in reference 3, the fuselage of circular cross section described in reference 5, and a fuselage of elliptical cross section were used. The combinations tested represented high-wing, low-wing, and midwing monoplanes. Some results from references 3 and 5 are included for comparison.

### APPARATUS AND MODELS

The tests were made in the NACA 7- by 10-foot wind tunnel with the regular six-component balance. The tunnel and the balance are described in references 6 and 7.

Plan views and elevations of the four wings are shown in figure 1. The tip plan form of the rectangular wing is composed of two quadrants of similar ellipses; for the other three wings, which are tapered 3:1, the ordinates of the ellipses have been expanded in proportion to the taper of the individual leading or trailing edges. The NACA 23012 profile is maintained to the ends of the wings and, in elevation, the maximum upper-surface ordinates are in one plane. The area of the rectangular wing is 3.917 square feet and the aspect ratio is 6.383; for the tapered wings, the area is 4.101 square feet and the aspect ratio is 6.097. The sweep angles of the tapered wings are  $-4.75^\circ$ ,  $4.75^\circ$ , and  $14.00^\circ$ . The wings were set at  $0^\circ$  incidence to the fuselage center line in all positions.

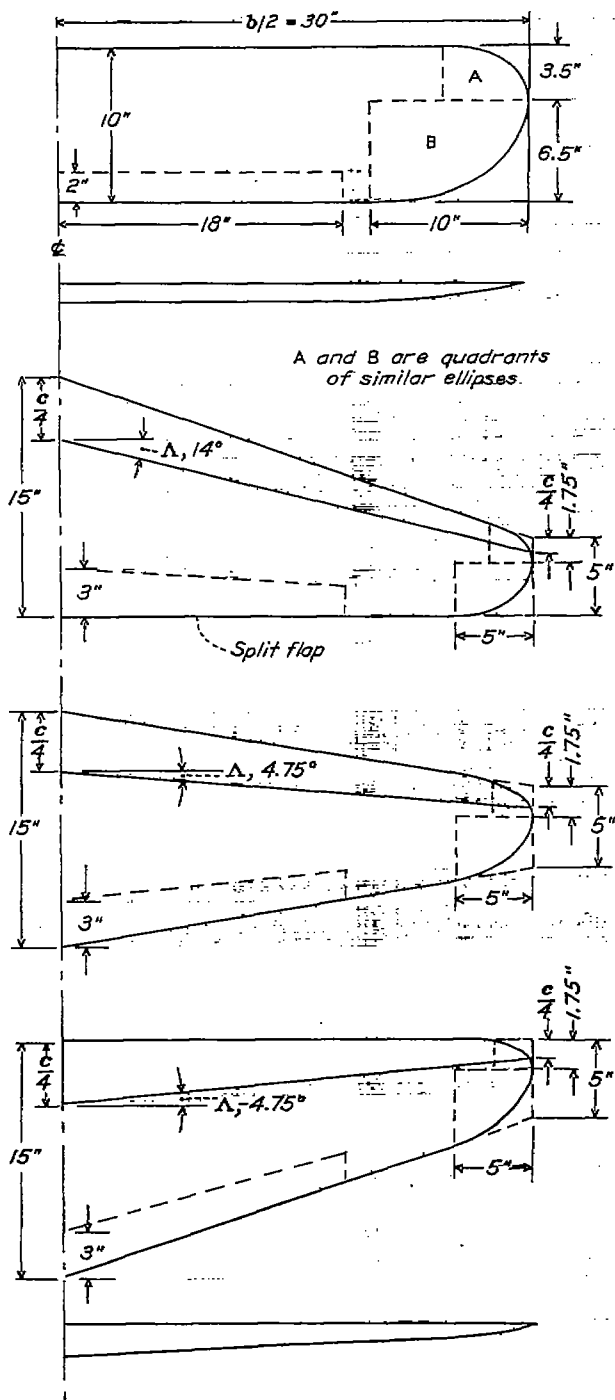


FIGURE 1.—Plan views and elevations of the NACA 23012 wings.

The two fuselages used are shown in figures 2 and 3 and the dimensions are given in table I. The maximum cross-sectional area of the two fuselages is the same. The circular fuselage, which was used for the tests reported in reference 5, was made from dimensions obtained from reference 8.

The fins were made to the NACA 0009 section and, in plan form, are representative of fins now in use. The area of the fin of the circular fuselage is 53.7 and that of the elliptical fuselage is 56.2 square inches. These areas are given to the center of the fuselage. The aspect ratios of the fins of the circular and of the elliptical fuselages are 2.20 and 2.26, respectively. The

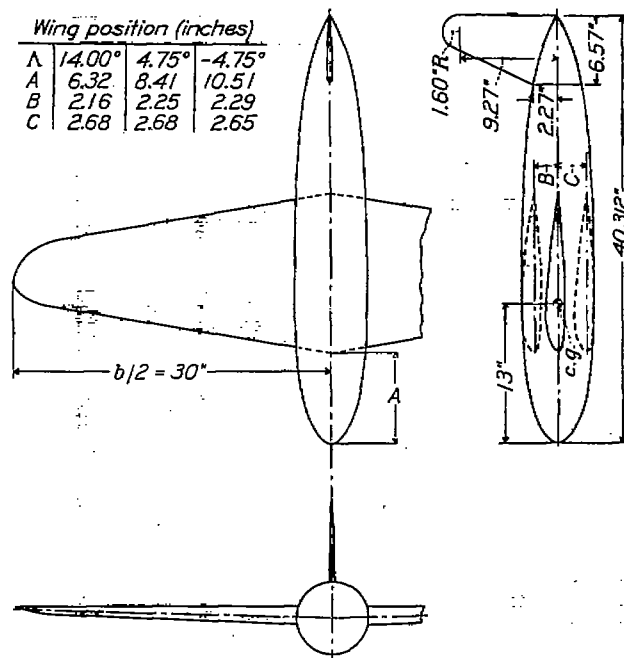


FIGURE 2.—Drawing of NACA 23012 wing in combination with circular fuselage and fin of NACA 0009 section.

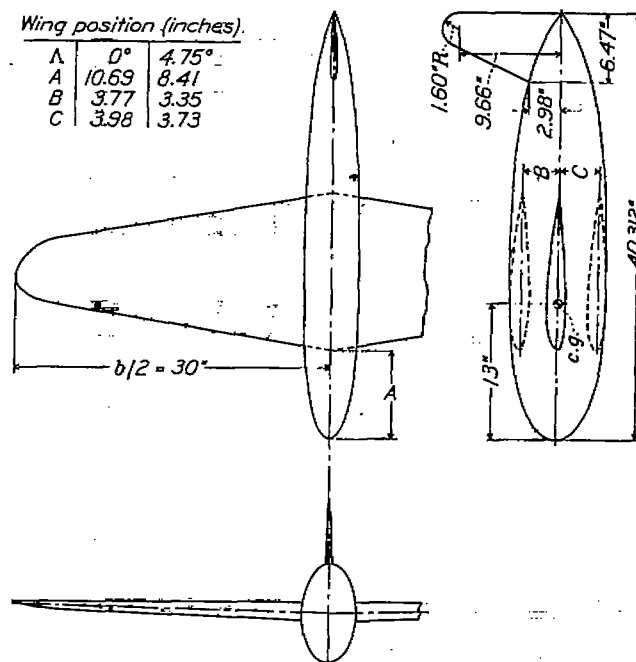
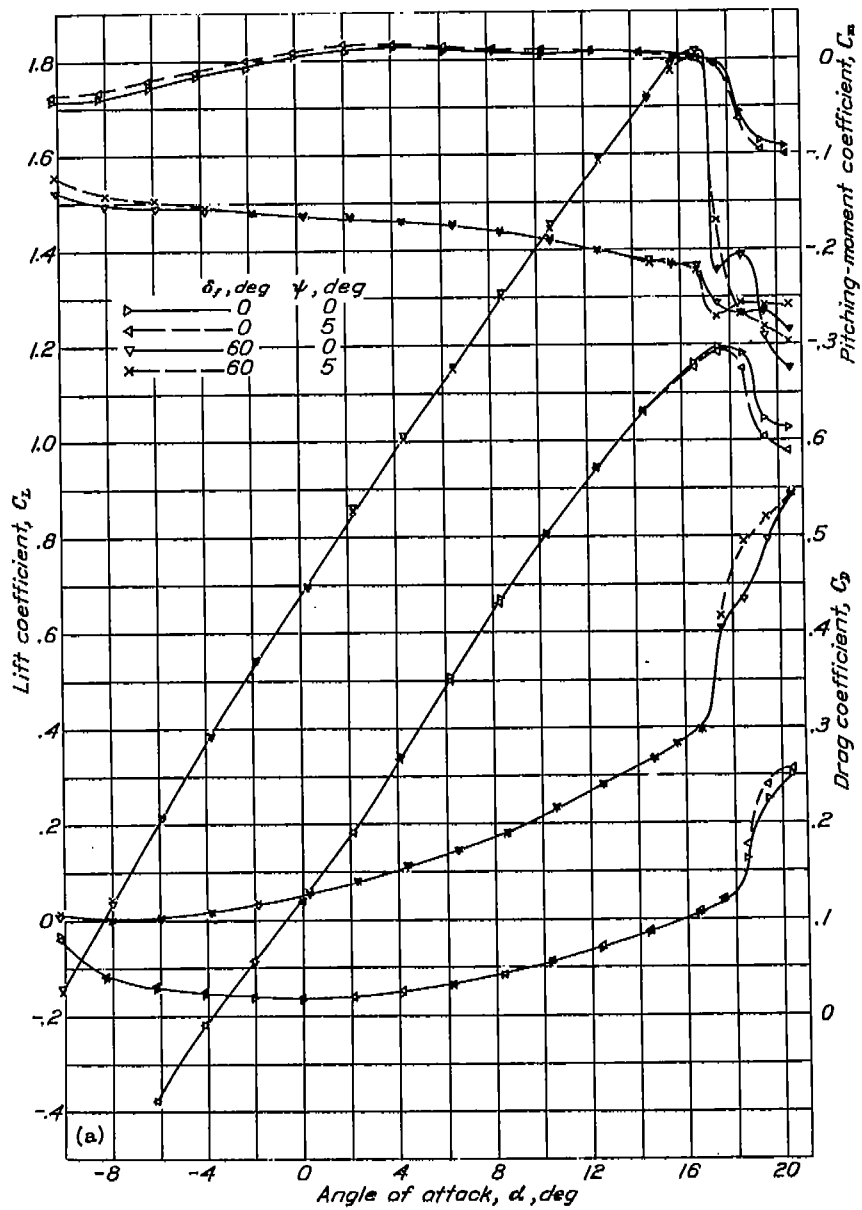


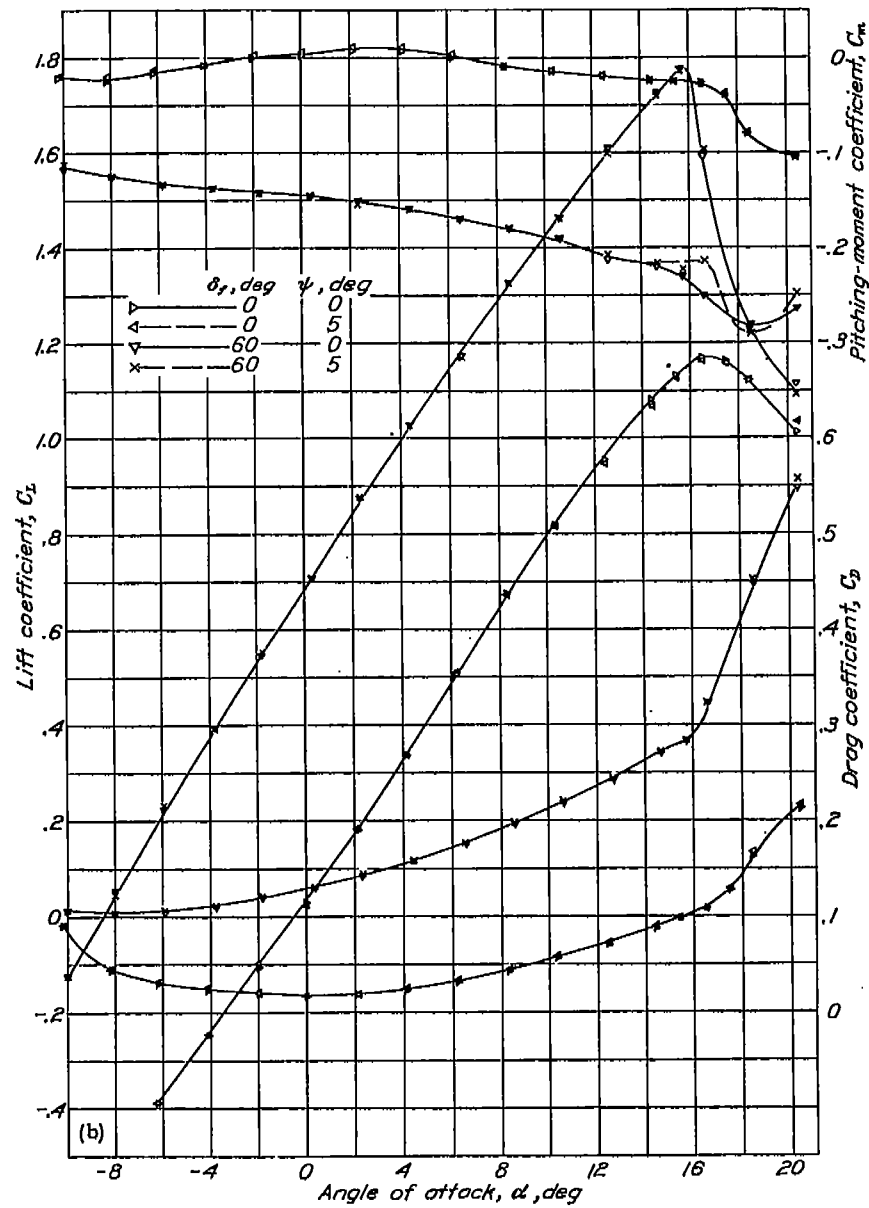
FIGURE 3.—Drawing of NACA 23012 wing in combination with elliptical fuselage and fin of NACA 0009 section.

distance from the assumed position of the center of gravity of the model to the trailing edge of the fin is 0.455 times the wing span.

The split flaps were made of 1/16-inch steel plates and, for the flap-deflected condition, were attached to the wing at an angle of 60°. The flaps have a chord 20 percent of the wing chord, are tapered with the wing chord, and extend over the inboard 60 percent of the span. For the midwing and the high-wing positions, the center section of the flap was cut away to allow for the fuselage. The gap between the flap and the fuselage was sealed for all tests.

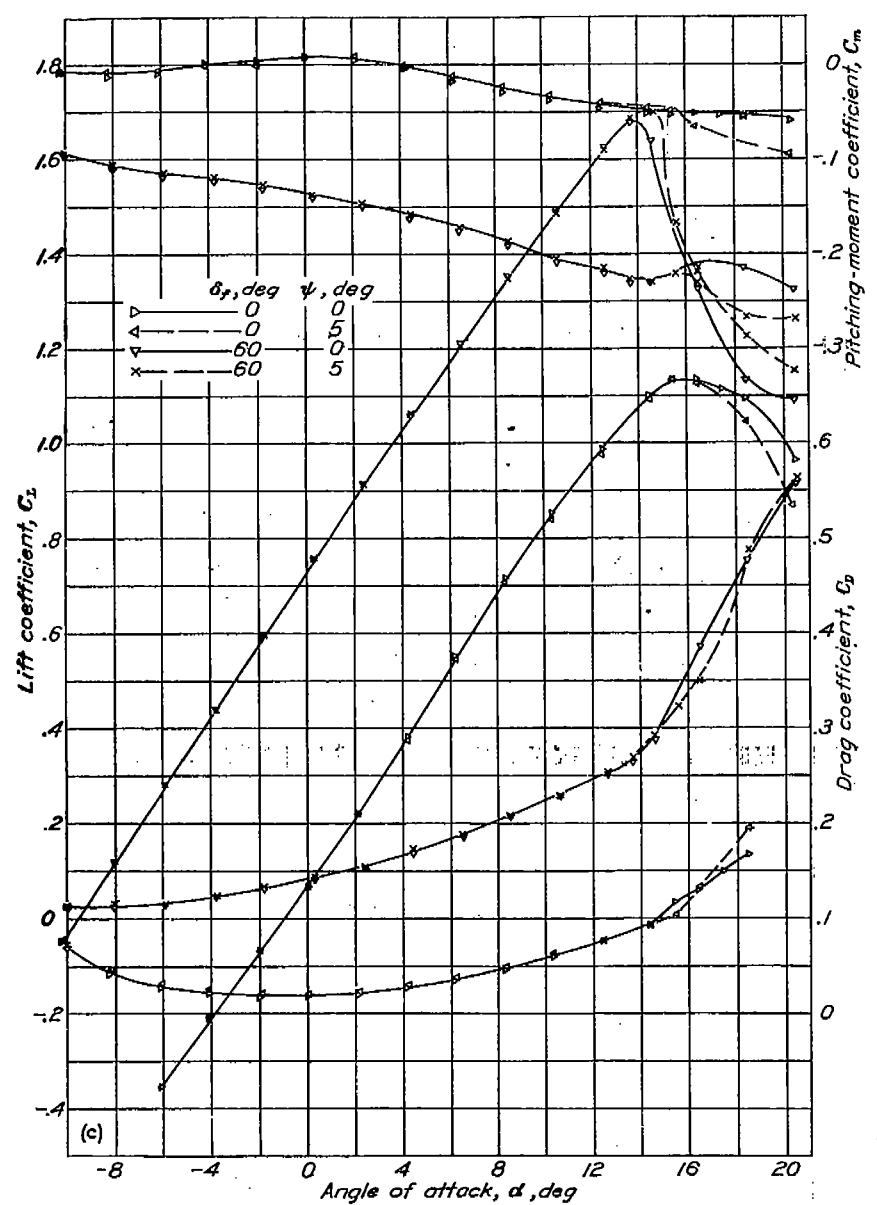


(a) Tapered wing;  $\Lambda, -4.76^\circ$ ; circular fuselage.

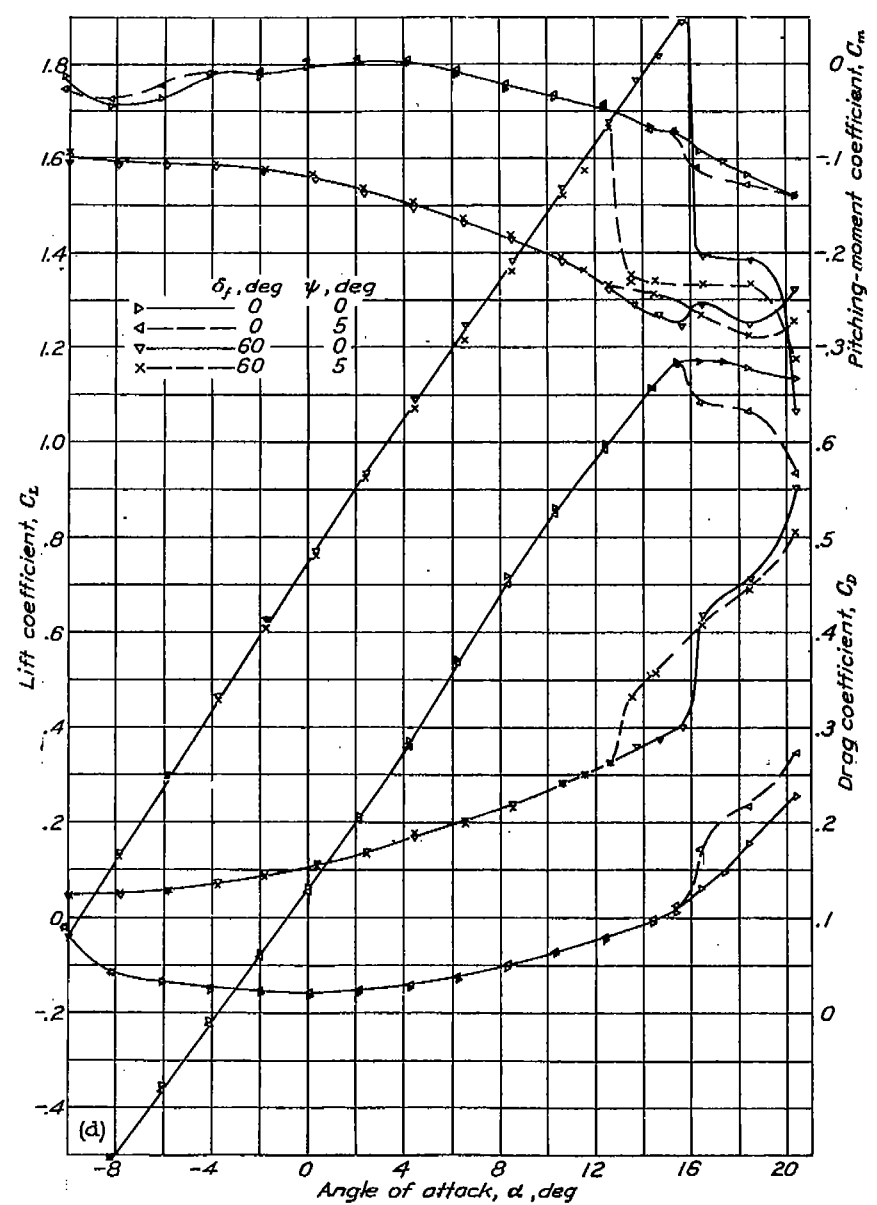


(b) Tapered wing;  $\Lambda, 4.76^\circ$ ; circular fuselage.

FIGURE 4.—Lift, drag, and pitching-moment coefficients of complete model as a high-wing monoplane.

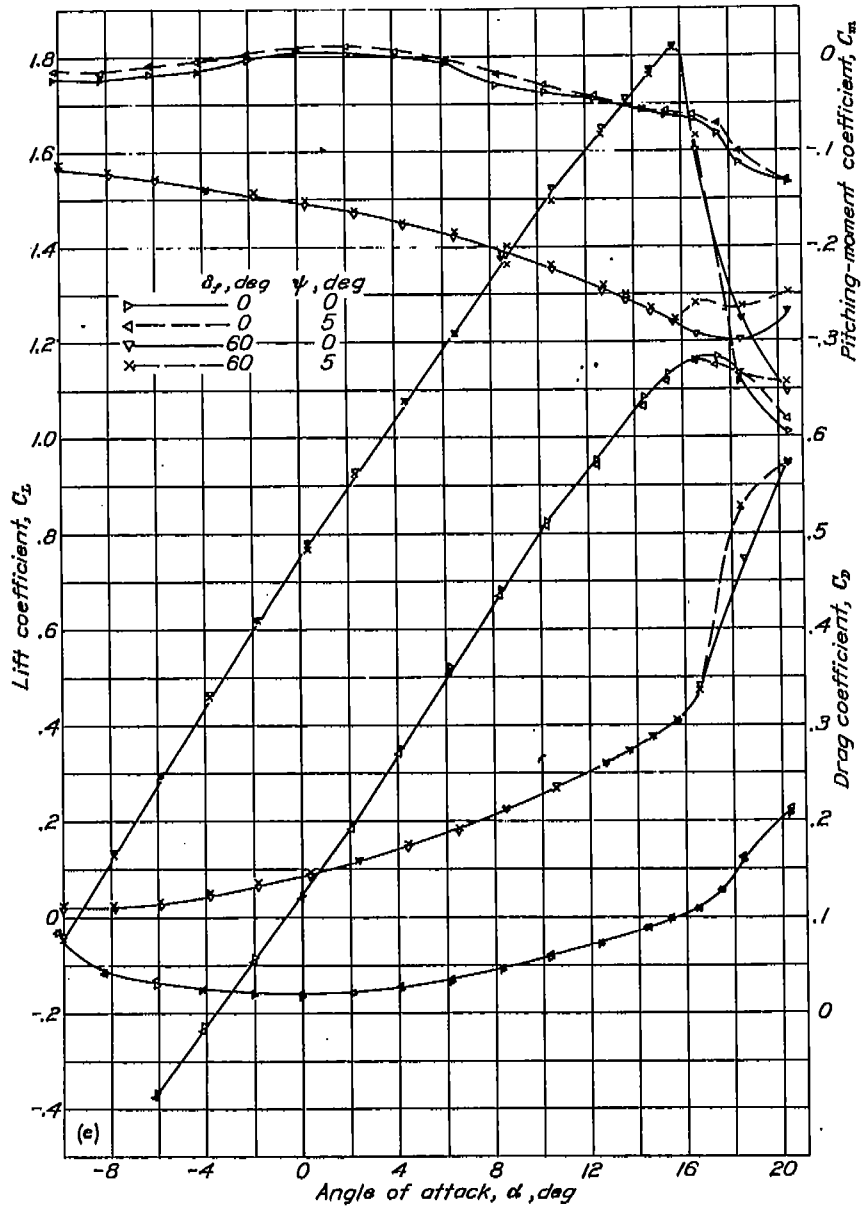


(c) Tapered wing;  $\Lambda$ , 14.00°; circular fuselage.



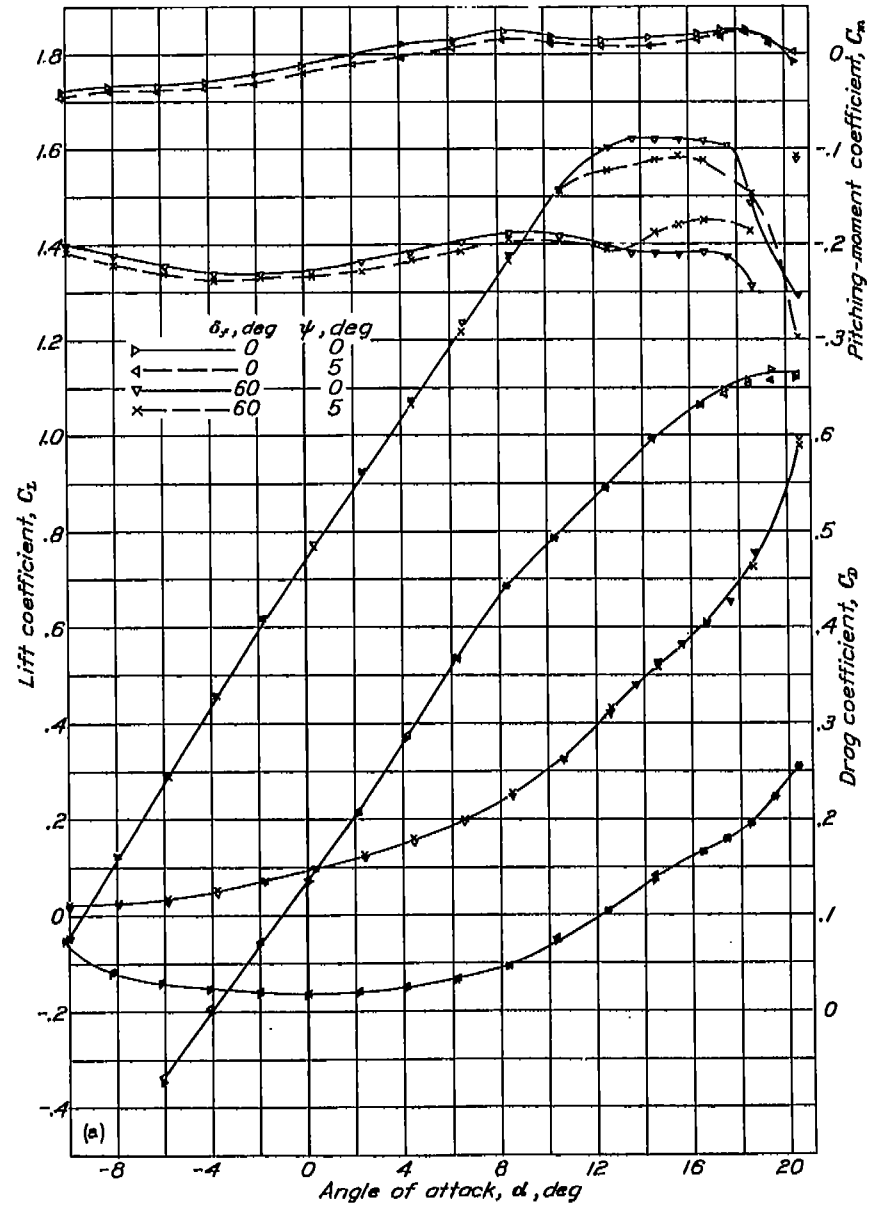
(d) Rectangular wing;  $\Lambda$ , 0°; elliptical fuselage.

FIGURE 4.—Continued.



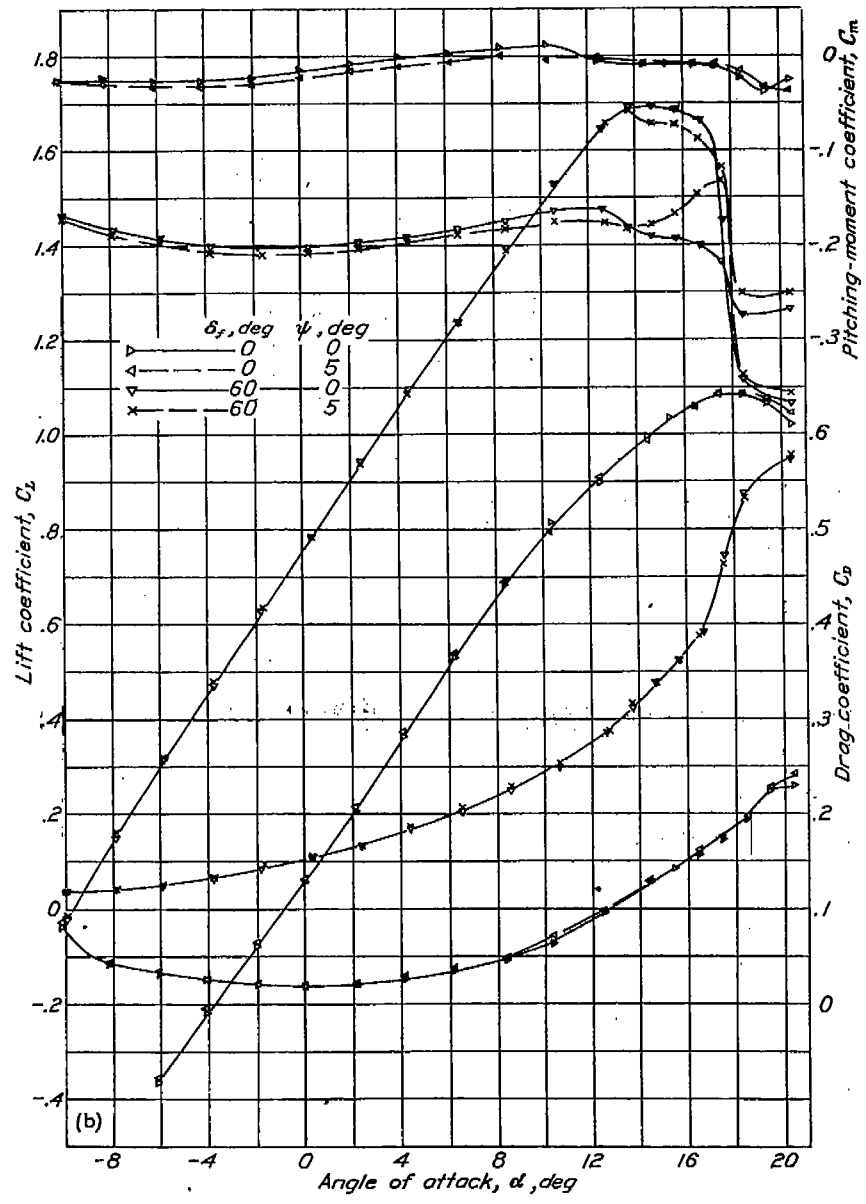
(e) Tapered wing;  $\Lambda=4.75^\circ$ ; elliptical fuselage.

FIGURE 4.—Concluded.

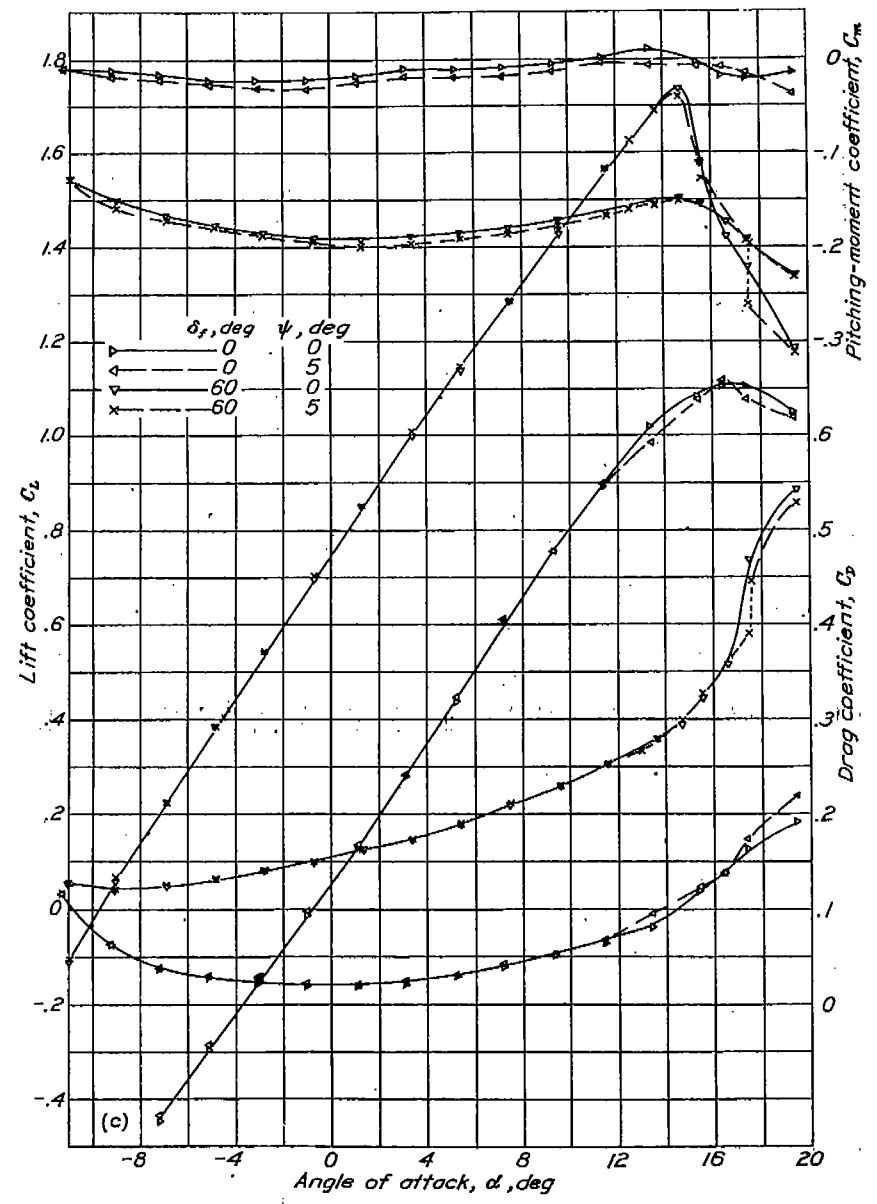


(a) Tapered wing;  $\Lambda=4.75^\circ$ ; circular fuselage.

FIGURE 5.—Lift, drag, and pitching-moment coefficients of complete model as a low-wing monoplane.



(b) Tapered wing;  $A, 4.75^\circ$ ; circular fuselage.



(c) Tapered wing;  $A, 14.00^\circ$ ; circular fuselage.

FIGURE 5.—Continued.

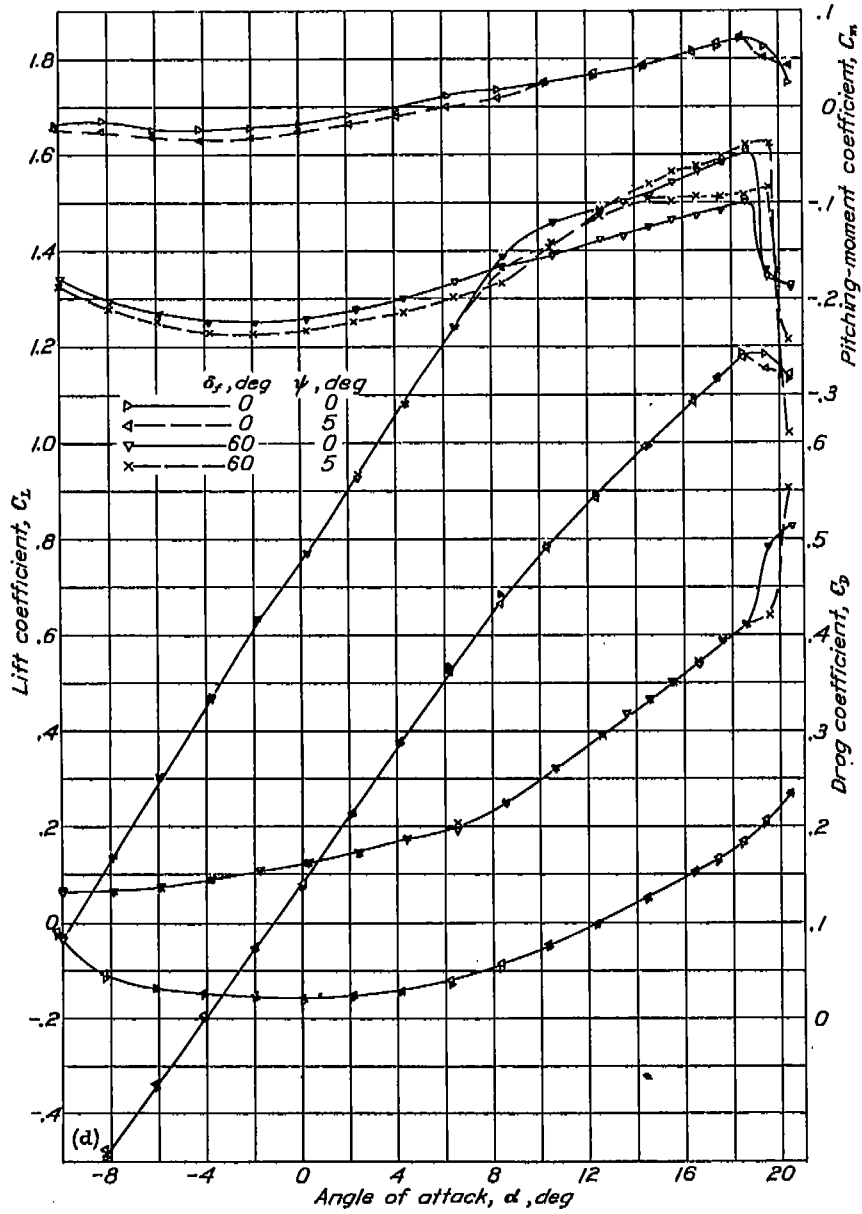
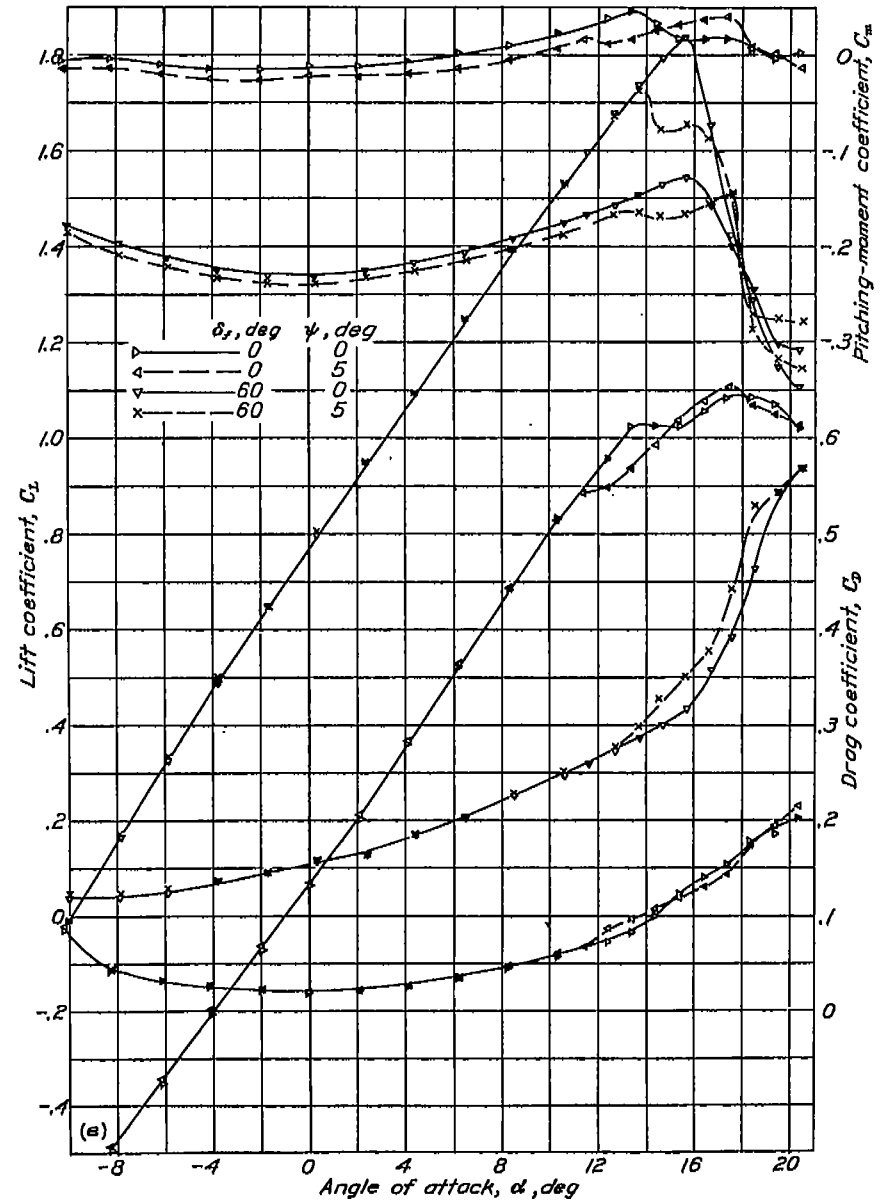
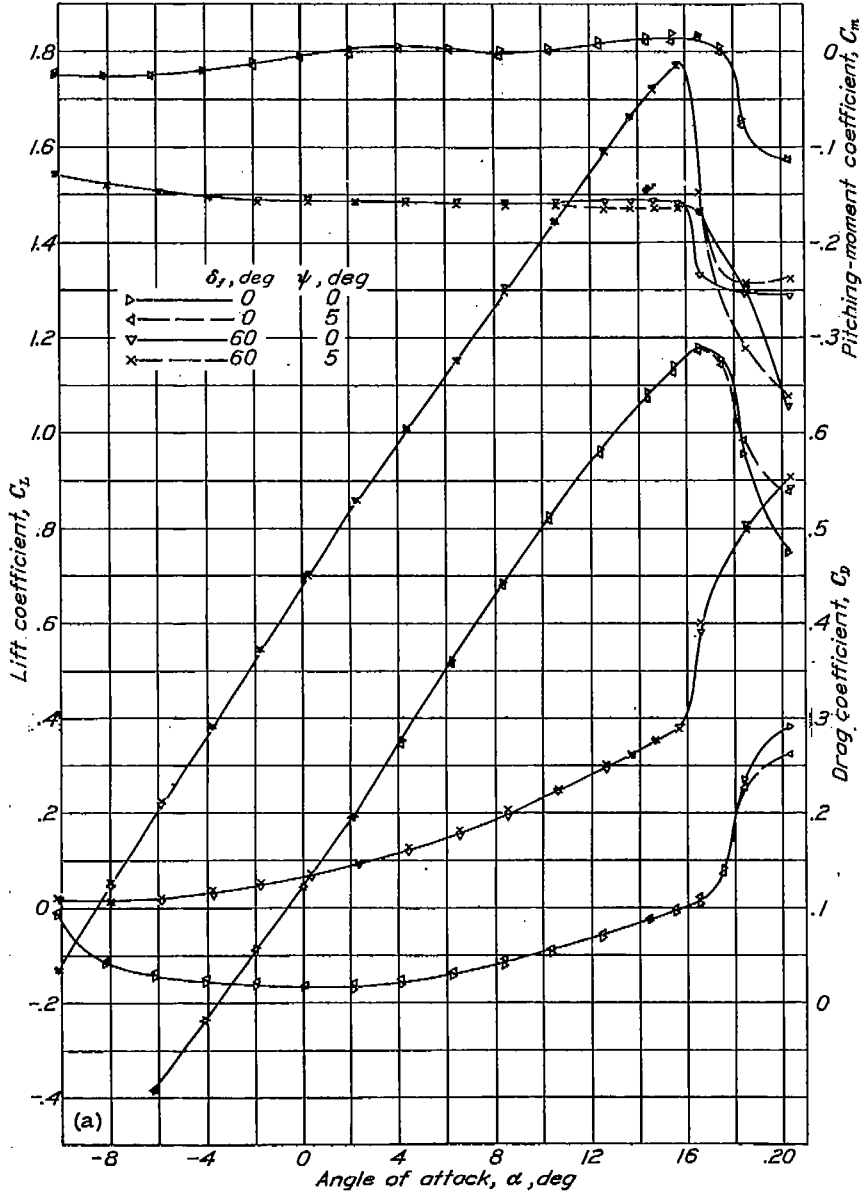
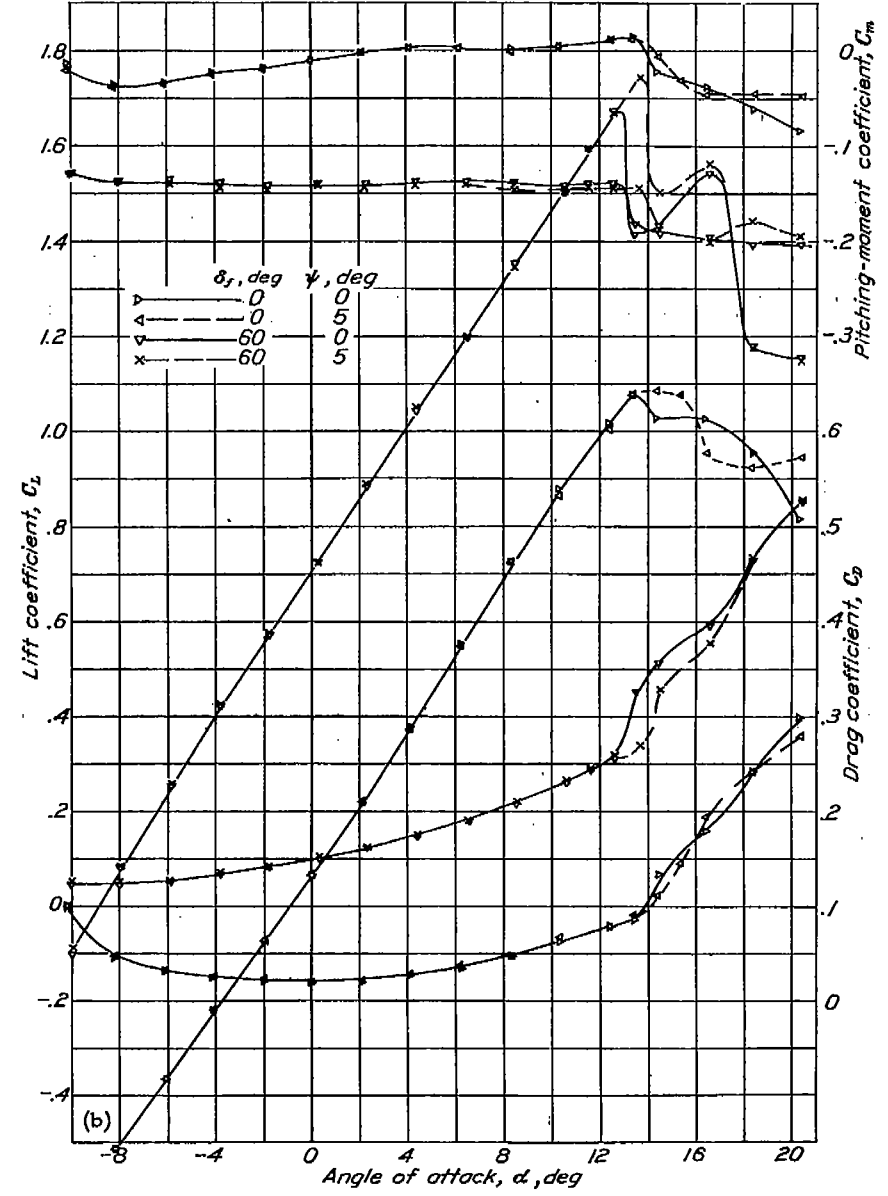
(d) Rectangular wing;  $\Lambda, 0^\circ$ ; elliptical fuselage.(e) Tapered wing;  $\Lambda, 4.73^\circ$ ; elliptical fuselage.

FIGURE 5.—Concluded.



(a) Tapered wing;  $\Lambda$ , 4.75°, circular fuselage.



(b) Rectangular wing;  $\Lambda$ , 0°, elliptical fuselage.

FIGURE 6.—Lift, drag, and pitching-moment coefficients of complete model as a midwing monoplane

TESTS

The tapered wings were tested with the circular fuselage, the rectangular wing having been previously tested in combination with this fuselage (reference 5). The rectangular wing in combination with the circular fuselage had been tested with 0° and 5° dihedral; for all other combinations, the wings were tested with 0° dihedral. The rectangular wing with no sweepback and the tapered wing with 4.75° sweepback were tested with the elliptical fuselage. Each fuselage was tested alone and in combination with the wings as a high-wing, a low-wing, and a midwing monoplane. For each combination, tests were made with and without the fin and with the flaps deflected 0° and 60°.

Tests were made with the model yawed -5°, 0°, and 5° through an angle-of-attack range from -10° to 20°. In addition, tests were made at angles of attack 1° and 4° below the stall through a yaw range of -10° to 15° to obtain additional information in the range of angles of attack shown to be critical in reference 5. All tests were made at a dynamic pressure of 16.37 pounds per square foot, which corresponds to an air speed of about 80 miles per hour under standard conditions. The test Reynolds number was about 609,000 based on a wing chord of 10 inches.

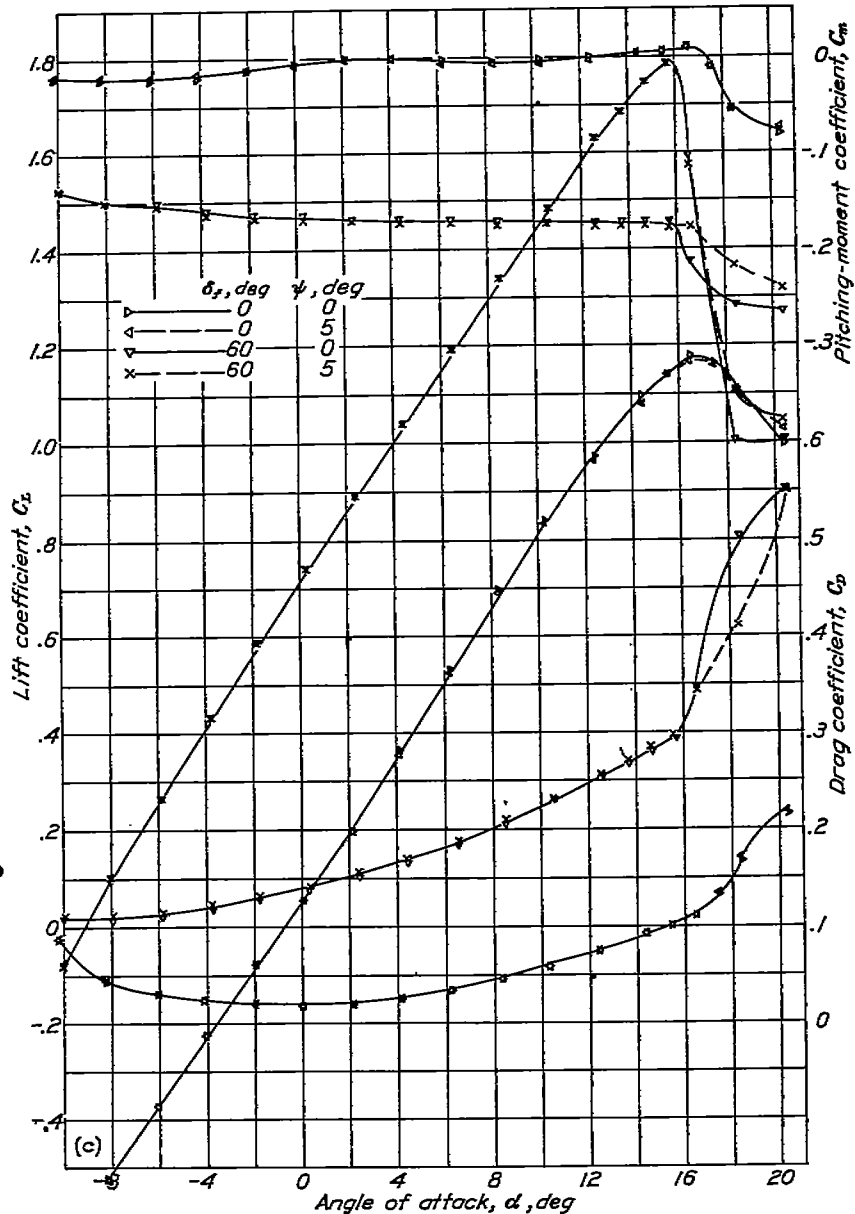
RESULTS

The data, with primes to indicate wind axes, are given in standard nondimensional coefficient form. The coefficients for the fuselages are based on the dimensions of the tapered wings.

- $C_L$  lift coefficient ( $L/qS$ )
- $C_D$  drag coefficient ( $D/qS$ )
- $C_{Y'}$  lateral-force coefficient ( $Y'/qS$ )
- $C_{Y'\psi}$  partial derivative of  $C_{Y'}$  with respect to  $\psi'$
- $C_l'$  rolling-moment coefficient ( $L'/qSb$ )
- $C_{l'\psi}$  partial derivative of  $C_l'$  with respect to  $\psi'$
- $C_m$  pitching-moment coefficient ( $M/qSc$ )
- $C_n'$  yawing-moment coefficient ( $N'/qSb$ )
- $C_{n'\psi}$  partial derivative of  $C_n'$  with respect to  $\psi'$

where

- $L$  lift
- $D$  drag
- $Y'$  lateral force
- $L'$  rolling moment
- $M$  pitching moment
- $N'$  yawing moment



(c) Tapered wing;  $\Lambda$ , 4.75°; elliptical fuselage.  
FIGURE 6.—Concluded.

- $q$  dynamic pressure ( $1/2 \rho V^2$ )
  - $V$  tunnel air velocity
  - $\rho$  air density
  - $S$  wing area
  - $b$  wing span
  - $\bar{c}$  average wing chord
  - $\psi'$  angle of yaw, degrees
- and
- $\alpha$  angle of attack
  - $\Lambda$  angle of sweep, degrees
  - $\Gamma$  dihedral angle between plane of maximum upper-surface ordinates and the  $X$ - $Y$  plane
  - $\delta_f$  flap deflection
  - $\Delta_1$  change in partial derivatives caused by wing-fuselage interference
  - $\Delta_2$  change in tail effectiveness caused by wing-fuselage interference

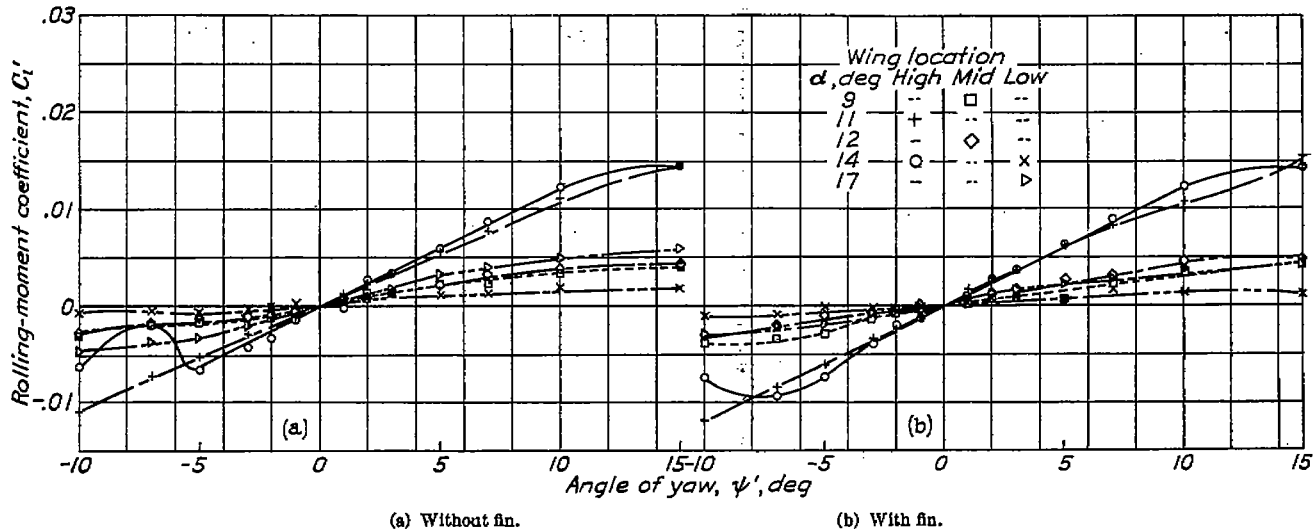


FIGURE 7.—Variation of rolling-moment coefficient with yaw. Elliptical fuselage and rectangular NACA 23012 wing;  $\Gamma, 0^\circ$ .

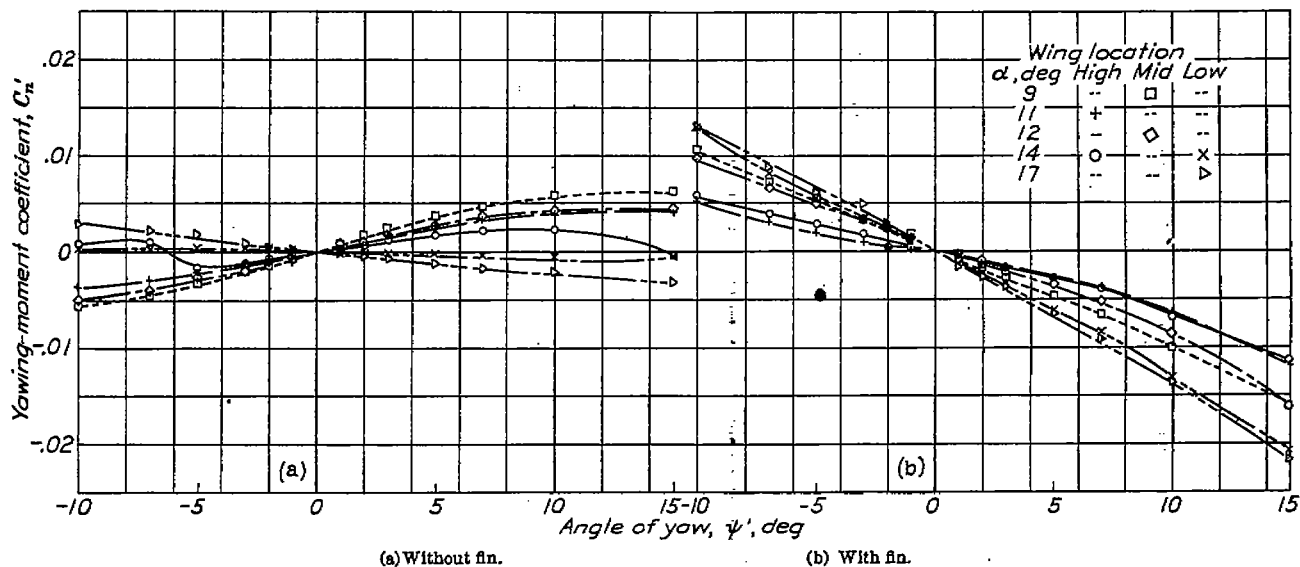


FIGURE 8.—Variation of yawing-moment coefficient with yaw. Elliptical fuselage and rectangular NACA 23012 wing;  $\Gamma, 0^\circ$ .

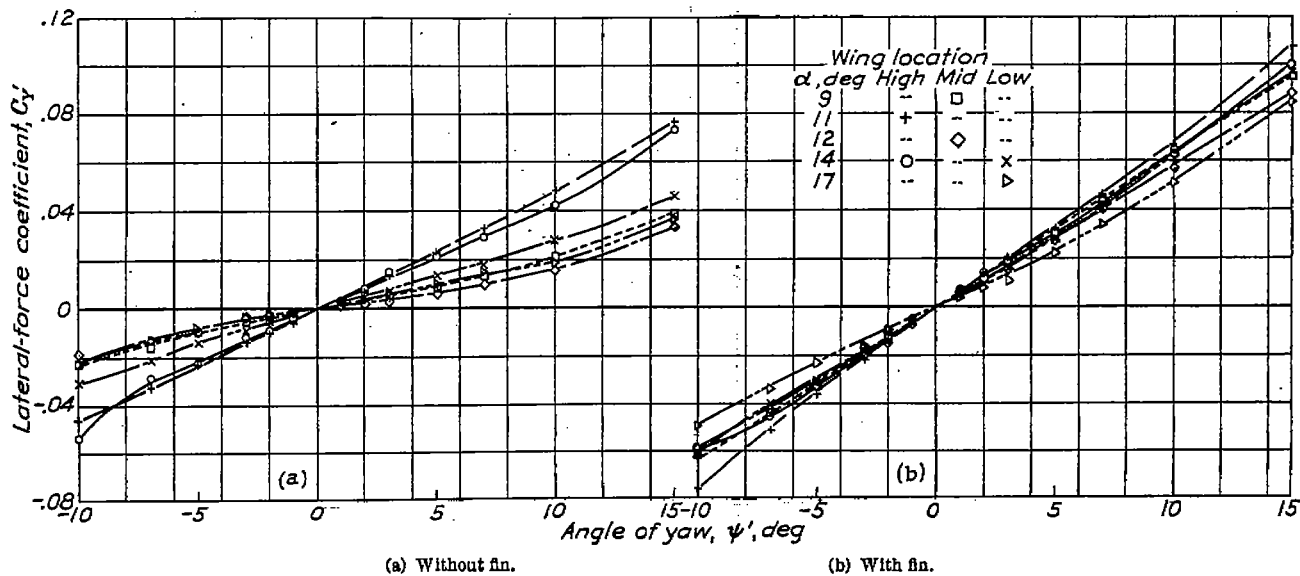


FIGURE 9.—Variation of lateral-force coefficient with yaw. Elliptical fuselage and rectangular NACA 23012 wing;  $\Gamma, 0^\circ$ .

The forces and the moments have been given with respect to the wind-tunnel system of axes that intersect in the model at the center-of-gravity location shown in figures 2 and 3.

Coefficients of lift, drag, and pitching moment are given in figures 4 to 6 for the high-wing, the low-wing, and the midwing combinations, respectively. The values of  $\alpha$  and  $C_D$  given in these figures were corrected to free air. The rolling-moment, the yawing-moment, and the lateral-force coefficients were corrected for initial asymmetry by deducting the values obtained without yaw from the values obtained with yaw; figures 7 to 9 are sample plots. The values of  $\alpha$  given

It should be noted that the pitching-moment coefficient was not zero for most of the tests. For such tests a correction to  $C_{i\psi}$  should be made by means of the following equation:

$$C_i = C_i' \cos \psi + \frac{c}{b} C_m \sin \psi$$

for small angles of  $\psi$

$$C_i = C_i' + \frac{c}{b} C_m \psi$$

By differentiation

$$C_{i\psi} = C_{i'\psi} + 0.0029 C_m$$

As an aid in the analysis of the results, it was thought desirable to isolate as far as possible the effects of wing-

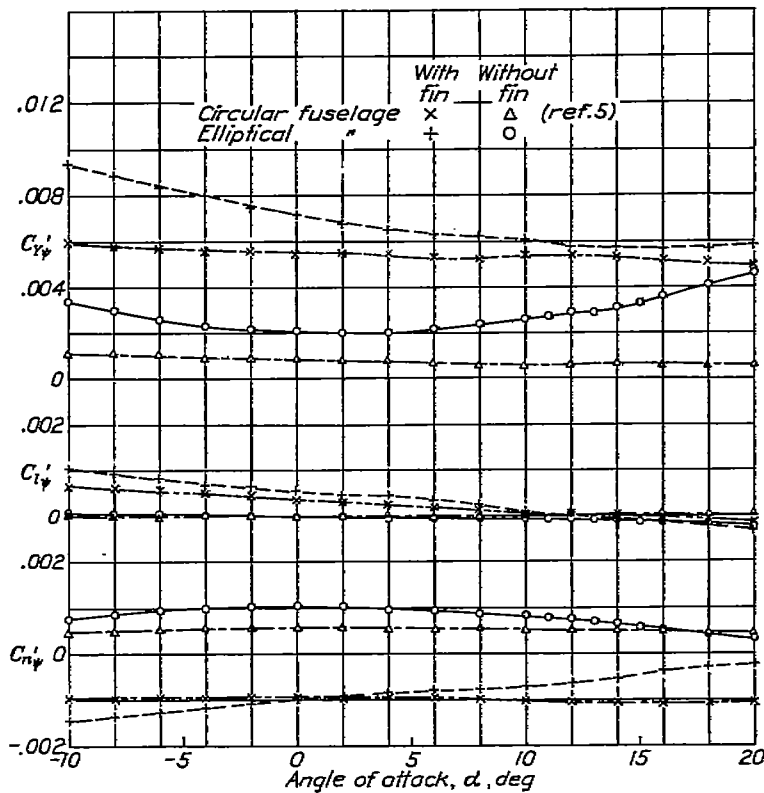


FIGURE 10.—Variation of  $C_{i\psi}'$ ,  $C_{n\psi}'$ , and  $C_{Y\psi}'$  with angle of attack. Circular and elliptical fuselage with and without fin.

in these and subsequent figures were not corrected; the data are therefore comparable with those of references 3 and 5.

The subscript  $\psi$  is used to denote the partial derivatives of the coefficients with respect to yaw angles. Thus  $C_{i\psi}'$ ,  $C_{n\psi}'$ , and  $C_{Y\psi}'$  are used instead of the more cumbersome expressions  $\partial C_i' / \partial \psi'$ ,  $\partial C_n' / \partial \psi'$ , and  $\partial C_Y' / \partial \psi'$ . The values of these derivatives were obtained from data measured at values of yaw of  $-5^\circ$  and  $5^\circ$  ( $\alpha$  variable) by assuming that the coefficients had a straight-line variation for the yaw range of  $-5^\circ$  to  $5^\circ$ . This method of obtaining slopes has been shown to be within the practical limits of accuracy except for angles of attack near the stall (reference 5). The slopes of  $C_{i\psi}'$ ,  $C_{n\psi}'$ , and  $C_{Y\psi}'$  are given in figure 10 for the fuselages; in figures 11 to 13 data for the wings are reproduced from reference 3.

fuselage interference. The data were therefore reduced to increments of  $C_{i\psi}'$ ,  $C_{n\psi}'$ , and  $C_{Y\psi}'$  caused by interference. The increments are subsequently called  $\Delta_1$  and  $\Delta_2$  and are written  $\Delta_1 C_{i\psi}'$ ,  $\Delta_1 C_{n\psi}'$ , etc. The value of  $\Delta_1$  is the difference between the values for the wing-fuselage combination without the fin and the sum of the values for the wing and the fuselage tested separately. Thus  $\Delta_1$  is the change in  $C_{i\psi}'$ ,  $C_{n\psi}'$ , and  $C_{Y\psi}'$  caused by wing-fuselage interference for the model without the tail. (See figs. 14 to 16.) The change in tail effectiveness caused by wing-fuselage interference is given by  $\Delta_2$ . As an example,  $\Delta_2 C_{n\psi}'$  is the change caused by wing-fuselage interference in  $C_{n\psi}'$  produced by the fin. The quantities  $\Delta_2 C_{i\psi}'$  and  $\Delta_2 C_{Y\psi}'$  are analogous to  $\Delta_2 C_{n\psi}'$ . (See figs. 17 to 19.)

In order to express the change in fin effectiveness caused by fuselage-fin interference, a third increment,

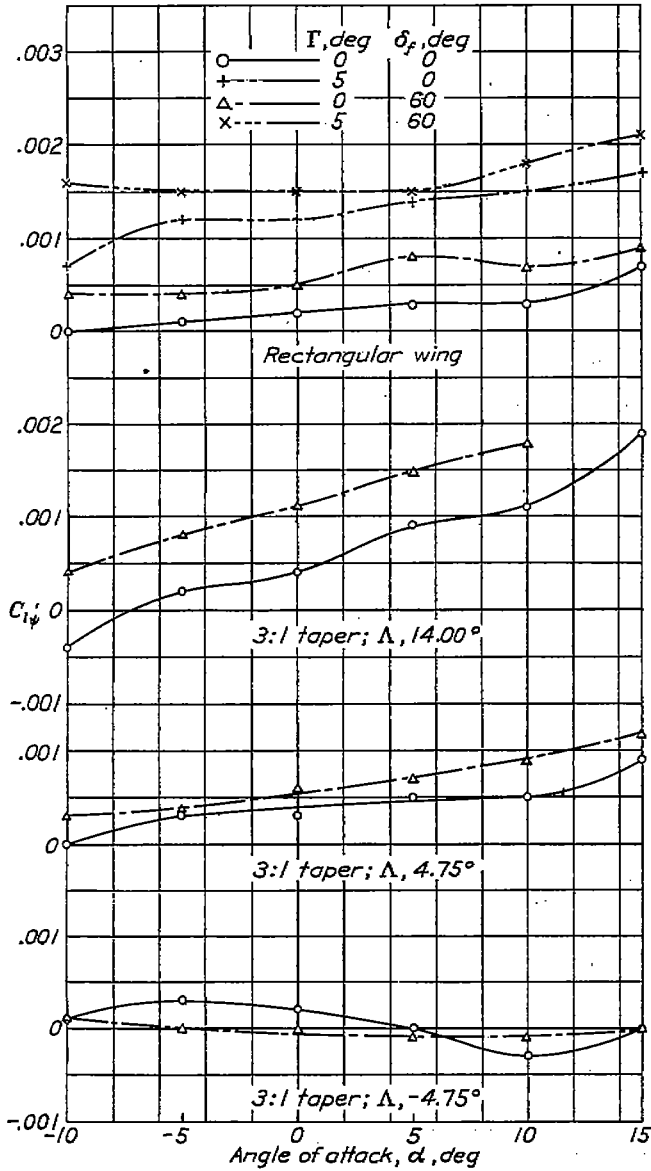


FIGURE 11.—Variation of  $C_{i\psi}'$  with angle of attack. NACA 23012 wings. (Data from reference 3.)

$\Delta_3$ , is necessary. The value of  $C_{n\psi}'$  for the complete model is then given by the following equation:

$$C_{n\psi}' = C_{n\psi}'(\text{wing}) + C_{n\psi}'(\text{fuselage}) + C_{n\psi}'(\text{fin}) + \Delta_1 + \Delta_2 + \Delta_3$$

It was impossible to evaluate  $\Delta_3$  because no tests were made of the fin alone. If the value for the complete model is desired, the following equation may be used instead of the equation just given:

$$C_{n\psi}' = C_{n\psi}'(\text{wing}) + C_{n\psi}'(\text{fuselage and fin}) + \Delta_1 + \Delta_2$$

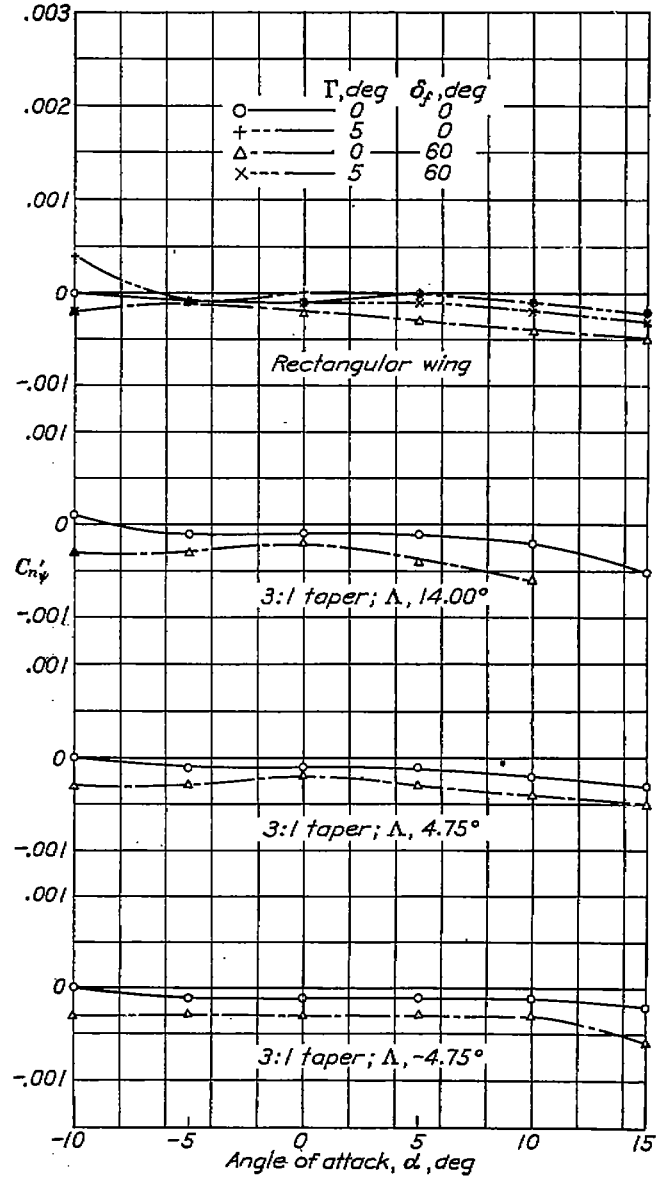


FIGURE 12.—Variation of  $C_{n\psi}'$  with angle of attack. NACA 23012 wings. (Data from reference 3.)

Values of  $C_{i\psi}'$  and  $C_{Y\psi}'$  for the complete model may be obtained in a similar manner.

### DISCUSSION

The application of theory to the problem of the influence of wing-fuselage interference on lateral-stability characteristics is difficult because of the complex flow involved. Several components of the flow and their probable effects will, however, be considered in a qualitative manner.

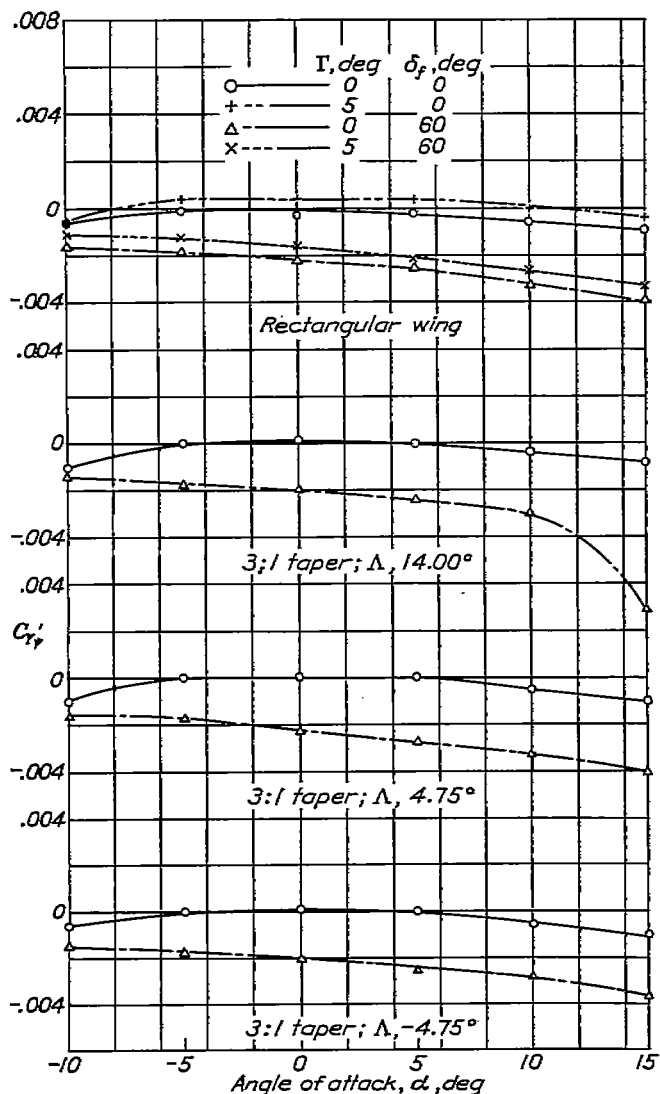


FIGURE 13.—Variation of  $C_{Y_p}$  with angle of attack. NACA 23012 wings. (Data from reference 3.)

Change in span load distribution is believed to be an important factor in wing-fuselage interference. Both the unsymmetrical flow resulting when the fuselage is yawed and the flow over and under the fuselage contribute to a change in the load distribution along the span of the wing.

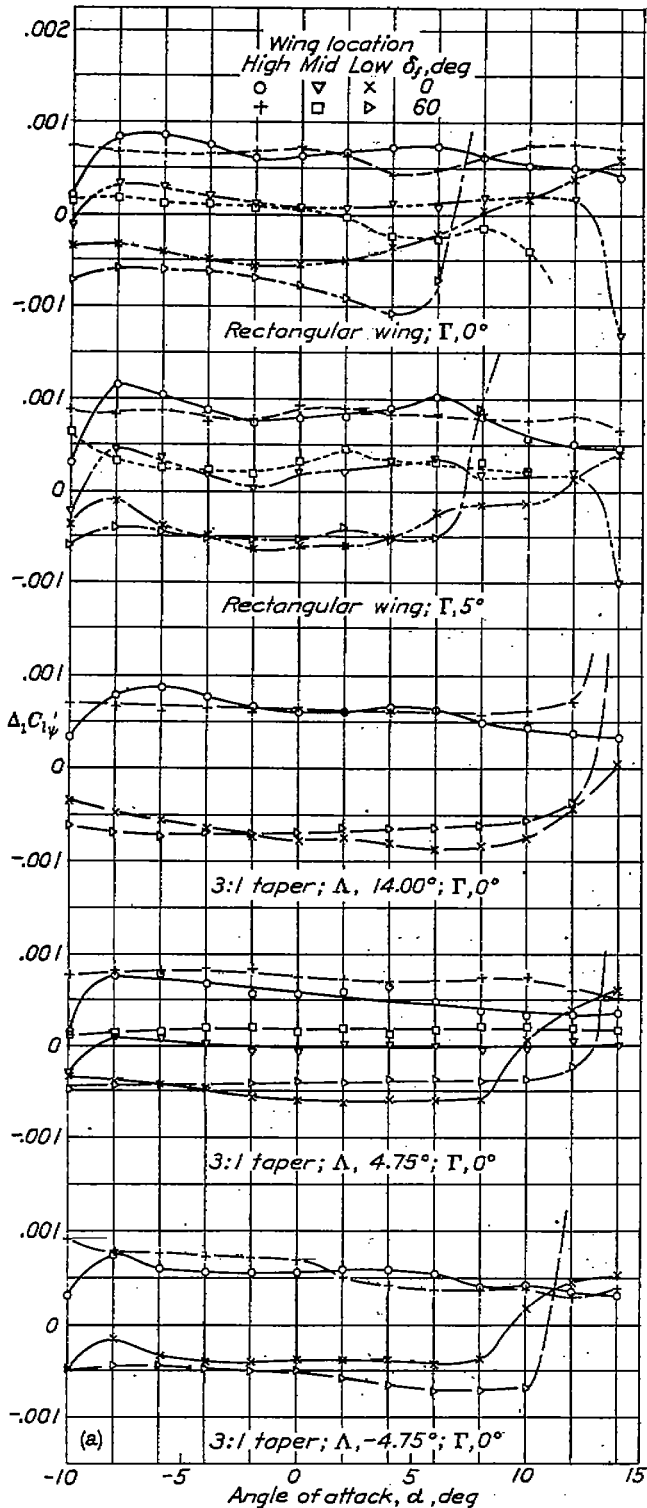
A region of increased pressure exists on the side of the fuselage toward the wind and a region of decreased pressure exists on the down-wind side. The flow about the wing will be modified depending on the position of the wing on the fuselage. With the wing in the high position, there will be an addition of lift on the side toward the wind and a corresponding reduction in lift on the down-wind side. Thus a rolling moment should

result that tends to raise the leading wing tip. It is easily seen that, with the wing in the low position, the change in loading would be such as to produce a rolling moment in the direction opposite to that obtained with the wing in the high position. With the wing in the midposition, this effect should be a minimum.

An additional change in span loading is brought about by local changes in wing angle of attack caused by the flow over and under the yawed fuselage. With the wing in the high position, the angle of attack of a portion of the wing near the fuselage is increased on the side toward the wind and is decreased on the down-wind side. An opposite change in angle of attack prevails with the wing in the low position; with the wing in the midposition, the change should be small.

Thus, when the model is yawed, the two interference factors considered should give an increment of rolling moment tending to raise the leading wing tip of a high-wing monoplane and to lower the leading wing tip of a low-wing monoplane. Longitudinal position of the wing on the fuselage should be an important factor in the change in span loading just discussed because of the fuselage load distribution.

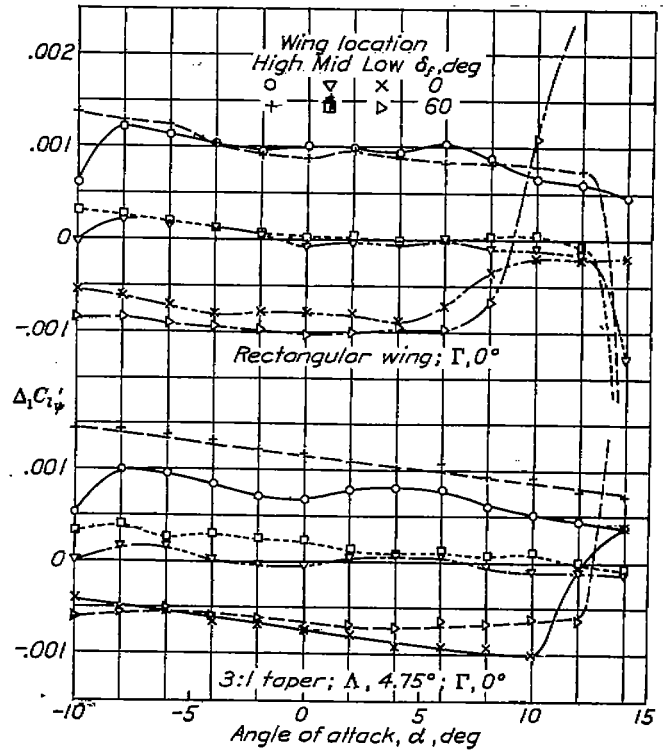
The presence of the wing exerts an appreciable influence on the flow about the fuselage. With either the high-wing or the low-wing monoplane in yaw the wing acts as a modified end plate, which should cause an increase in lateral force. The presence of the wing should also change the fuselage load distribution. Thus the longitudinal position of the wing on the fuselage should affect both the magnitude and the center of pressure of the lateral force and, consequently, the magnitude of the unstable yawing moment of the fuselage. The vortex field is apparently affected by interference, which results in an induced lateral flow at the tail. When the fuselage alone is yawed, vortices are shed at the top and the bottom of the fuselage somewhat like the tip vortices of a wing, the strength of these vortices increasing with increase in lateral force. If a wing is placed on the fuselage in the high or the low position, the lateral force should be increased because of the end-plate effect and the vortices should increase in strength. With the wing in the low position, however, the vortices shed from the bottom of the fuselage are so affected by the wing that the induced lateral flow near the bottom of the fuselage is greatly reduced. Similarly, with the wing in the high position, the induced lateral flow is decreased at the top of the fuselage. These characteristics have been noted in visual observations of the flow by means of tufts.



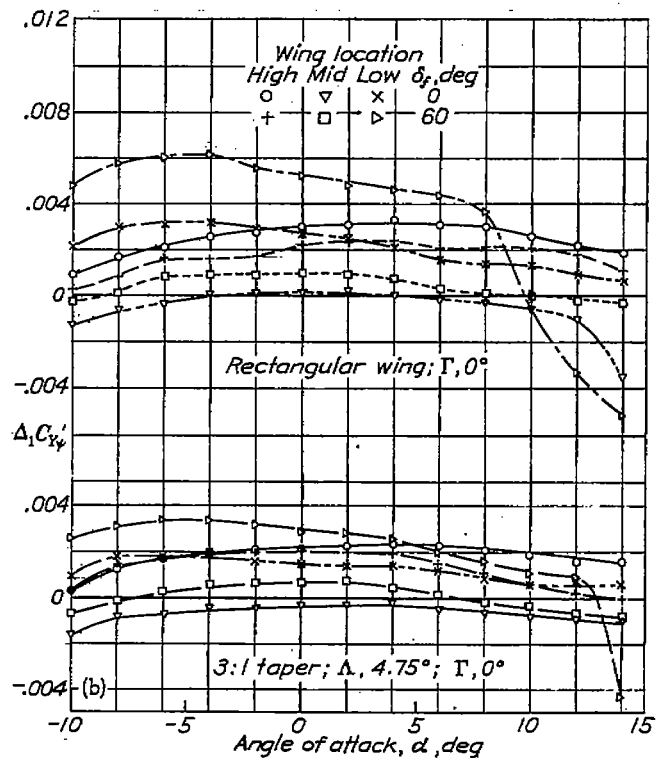
(a) Circular fuselage. (Data for rectangular wing was obtained from reference 5.)  
 FIGURE 14.—Increment of  $C_{l'\psi}$  due to wing-fuselage interference. NACA 23012 wings.

A diagrammatic sketch showing a probable distribution of the vortex field caused by interference is given in figure 20 for the low-wing monoplane.

From the foregoing discussion, it is seen that the induced lateral velocity acts to increase the effective angle of attack of the fin of a low-wing monoplane and to reduce the angle of attack of the fin of a high-wing monoplane.



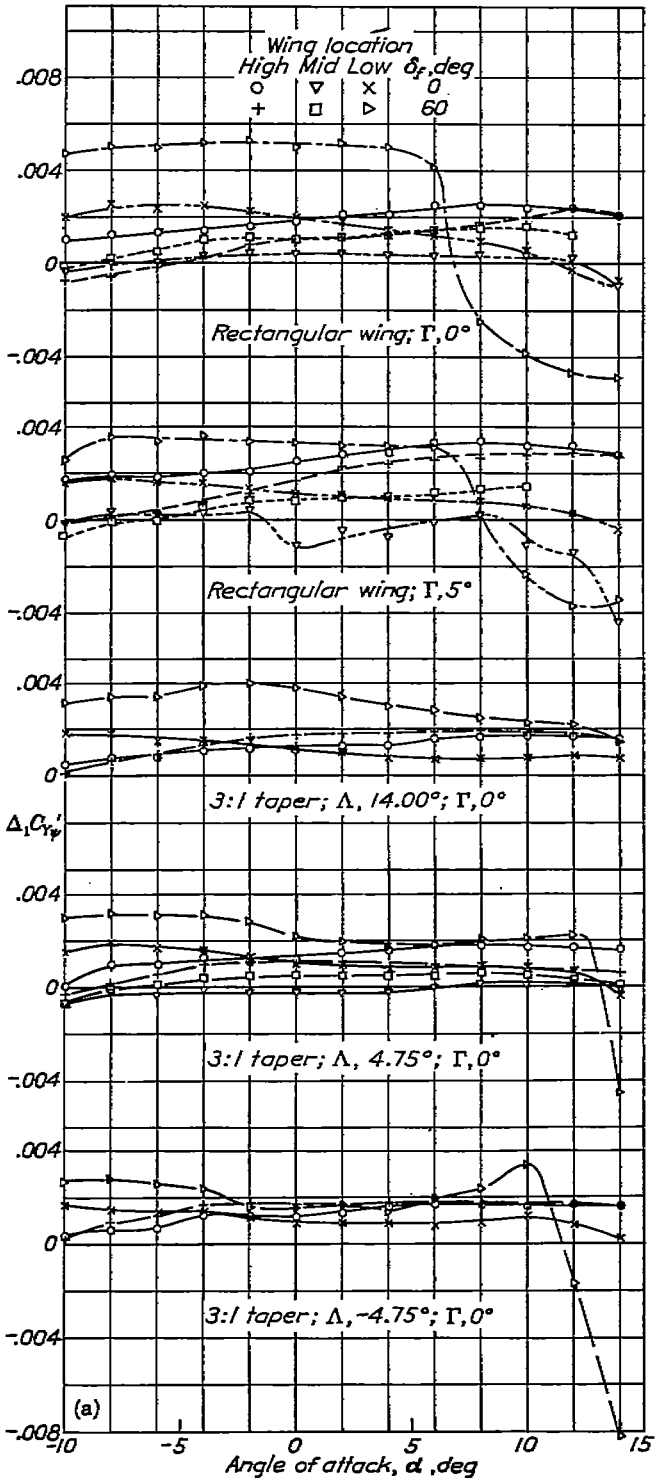
(b) Elliptical fuselage.  
 FIGURE 14.—Concluded.



(b) Elliptical fuselage.  
 FIGURE 15.—Increment of  $C_{y'\psi}$  due to wing-fuselage interference. NACA 23012 wings.

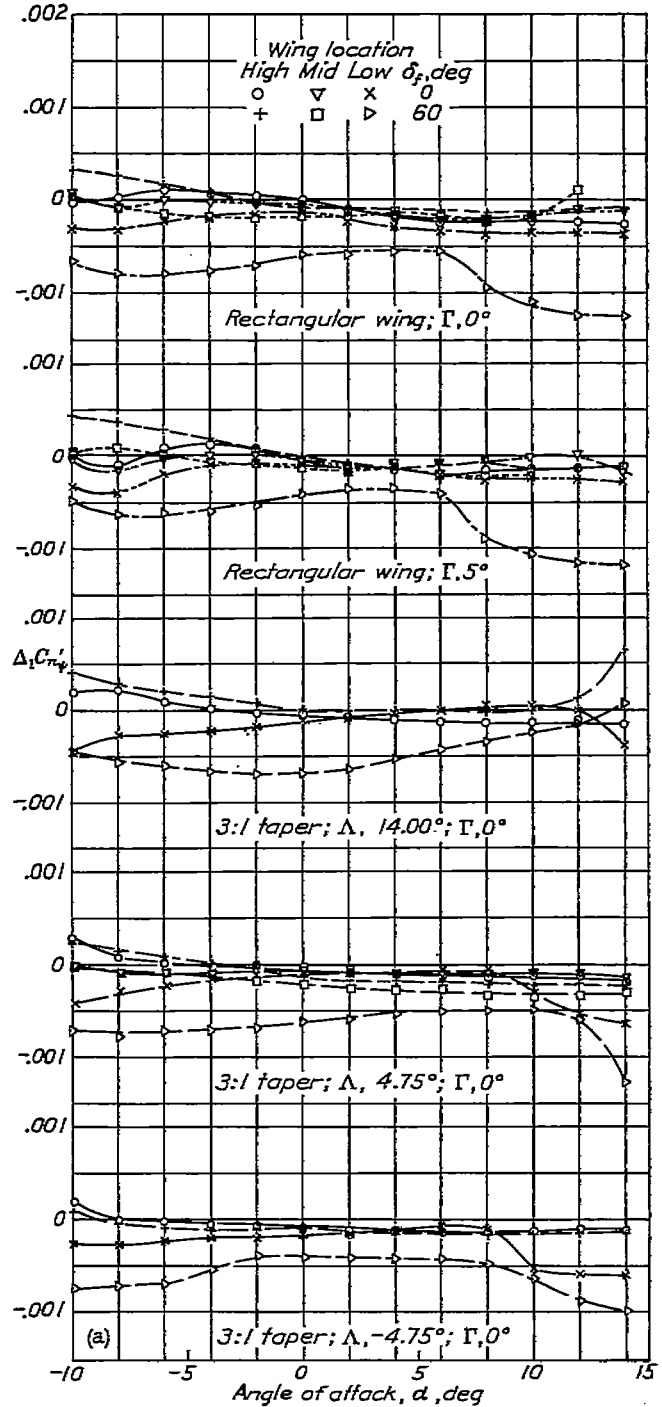
COMPONENT PARTS

Fin and fuselage.—The values of  $C_{l'\psi}$ ,  $C_{n'\psi}$ , and  $C_{y'\psi}$ , for the fuselages with the fins are given in figure 10. The results for the circular fuselage were obtained from reference 5 and are included here for comparison with the data for the elliptical fuselage. The value of  $C_{y'\psi}$



(a) Circular fuselage. (Data for rectangular wing was obtained from reference 5.)  
 FIGURE 15.—Increment of  $C'_{Y\psi}$  due to wing-fuselage interference. NACA 23012 wings.

was computed for a wing of the same aspect ratio as the fin from the data given in figure 4 of reference 9. The increase in  $C'_{Y\psi}$  produced by the fin is about 10 percent greater than this computed value. The change in  $C'_{i\psi}$  with angle of attack is of the order expected from the change in  $C'_{Y\psi}$  produced by the fin and the vertical-tail position; the change in  $C'_{n\psi}$  produced by

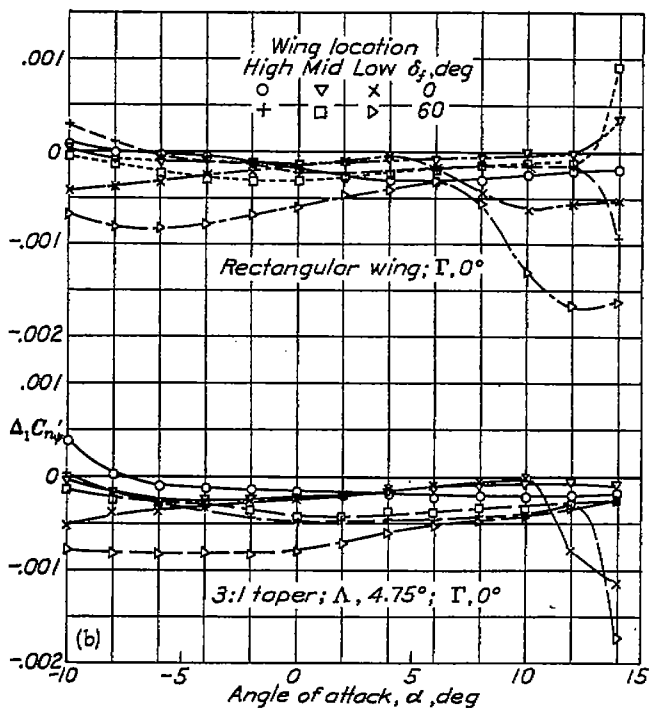


(a) Circular fuselage. (Data for rectangular wing was obtained from reference 5.)  
 FIGURE 16.—Increment of  $C'_{n\psi}$  due to wing-fuselage interference. NACA 23012 wings.

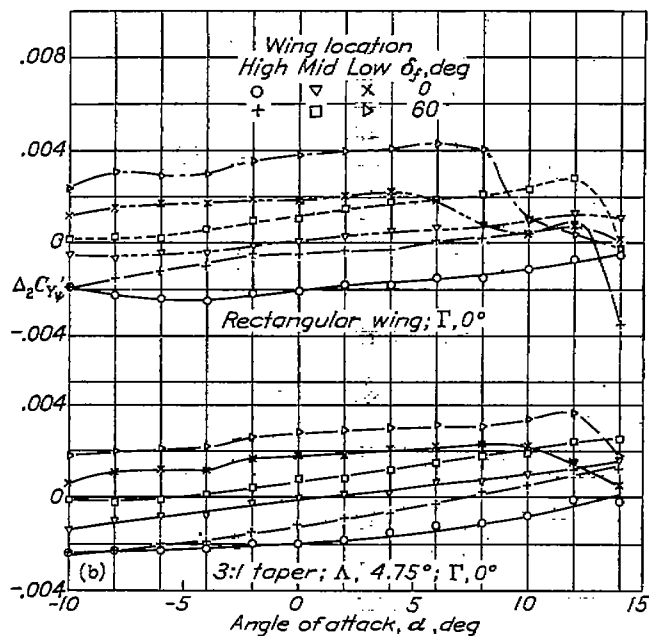
the fin is in the order of 80 percent of that expected from the change in  $C'_{Y\psi}$  and the tail length.

The relationships of  $C'_{i\psi}$ ,  $C'_{n\psi}$ , and  $C'_{Y\psi}$  previously given apply also for the elliptical fuselage and the fin except that the value of  $C'_{n\psi}$  produced by the fin is about equal to that computed from the increase in  $C'_{Y\psi}$  produced by the fin and the tail length.

Angle of attack is an important factor in determining the stability characteristics of the elliptical fuse-

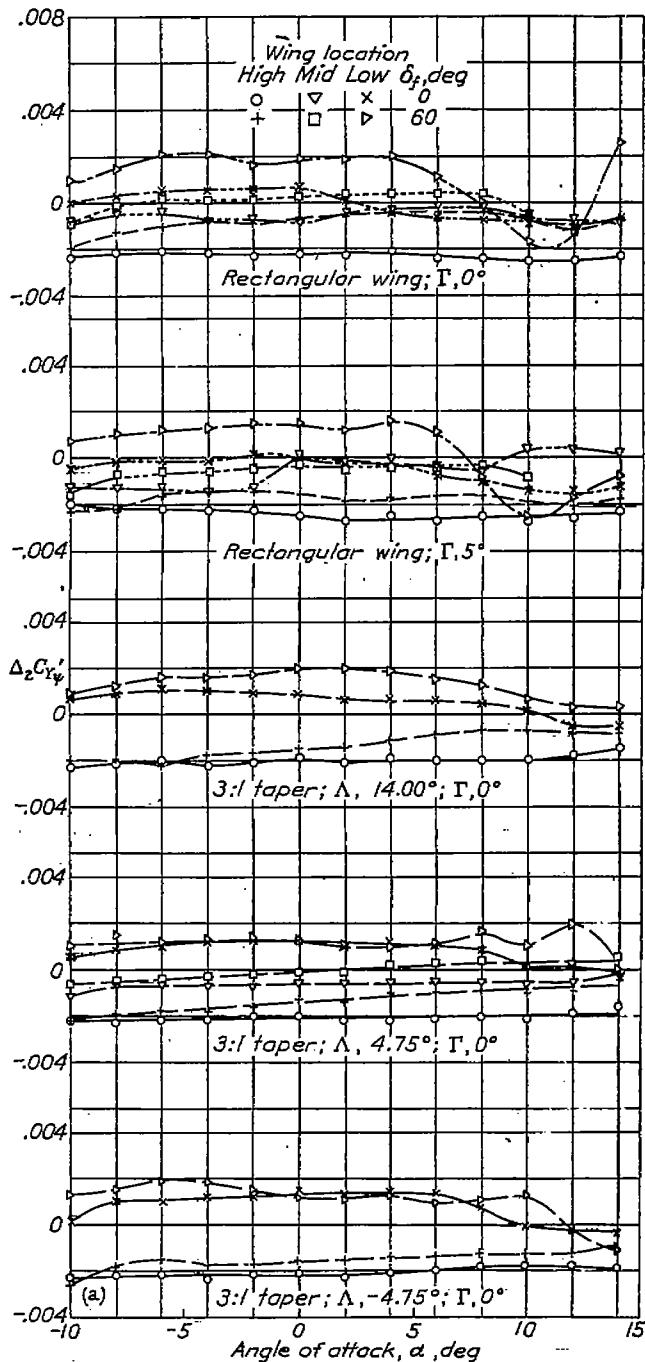


(b) Elliptical fuselage.  
FIGURE 16.—Concluded.



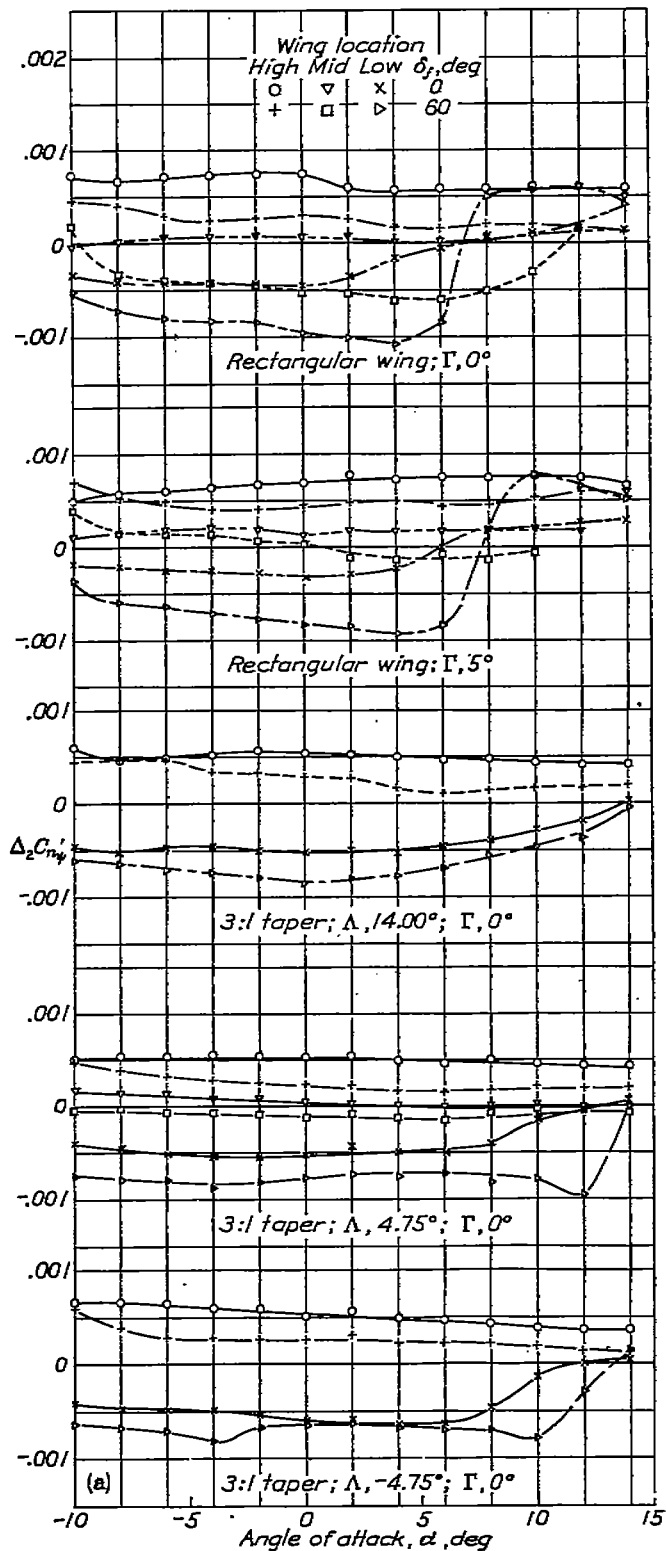
(b) Elliptical fuselage.  
FIGURE 17.—Concluded.

lage. At 0° angle of attack, the values of  $C_{Y'\psi}$  and  $C_{n'\psi}$  for the elliptical fuselage are nearly twice as large as those for the circular fuselage. At this angle of attack,  $C_{Y'\psi}$  is a minimum and  $C_{n'\psi}$  is a maximum. A change in angle of attack in either direction from 0° is accompanied by a marked increase in  $C_{Y'\psi}$  and by an appreciable reduction in unstable yawing moment, indicating a movement of the center of pressure toward the rear.



(a) Circular fuselage. (Data for rectangular wing was obtained from reference 5.)  
FIGURE 17.—Effect of wing-fuselage interference on  $C_{Y'\psi}$  due to fin. NACA 23012 wings.

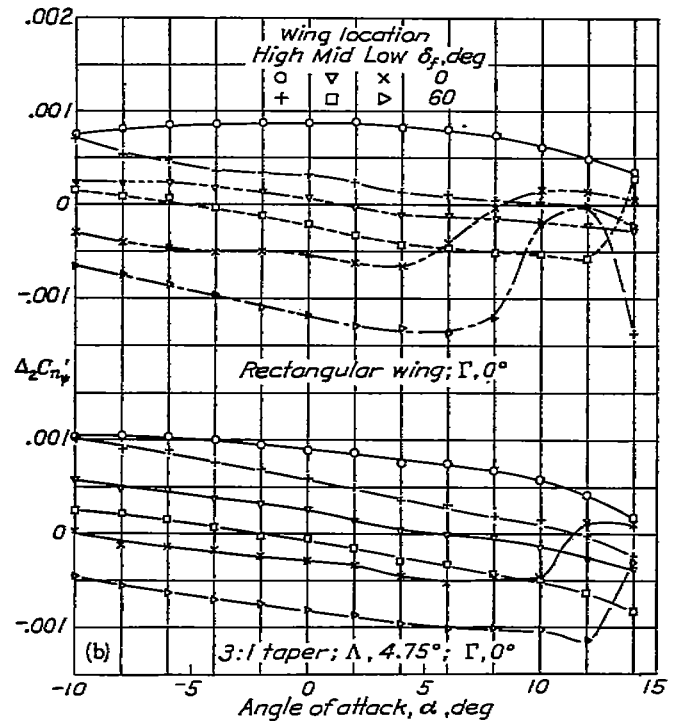
The increment of  $C_{Y'\psi}$  produced by the fin is very nearly the same for both fuselages at 0° angle of attack. An increase in angle of attack causes a decrease in the effectiveness of the fin of the elliptical fuselage. A study of the air flow by means of tufts indicated that this effect is probably the result of a partial blanketing of the fin by the fuselage. This effect becomes more pronounced as the angle of attack is increased. These results show that fuselage shape may be an important factor in determining the effectiveness of the fin.



(a) Circular fuselage. (Data for rectangular wing was obtained from reference 5.)

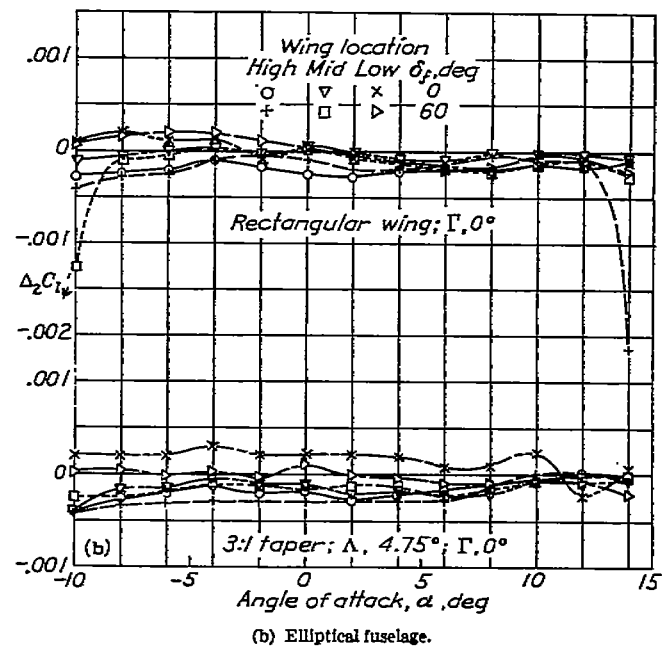
FIGURE 18.—Effect of wing-fuselage interference on  $C_{x'_{\psi}}$  due to fin. NACA 23012 wings.

Wings.—The results for the wings alone are taken from reference 3 and the general conclusions given therein will be briefly reviewed. (See figs. 11 to 13.) An increase in dihedral causes an increase in  $C_{i'_{\psi}}$  of about 0.0002 per degree, has little effect on  $C_{x'_{\psi}}$ , and



(b) Elliptical fuselage.

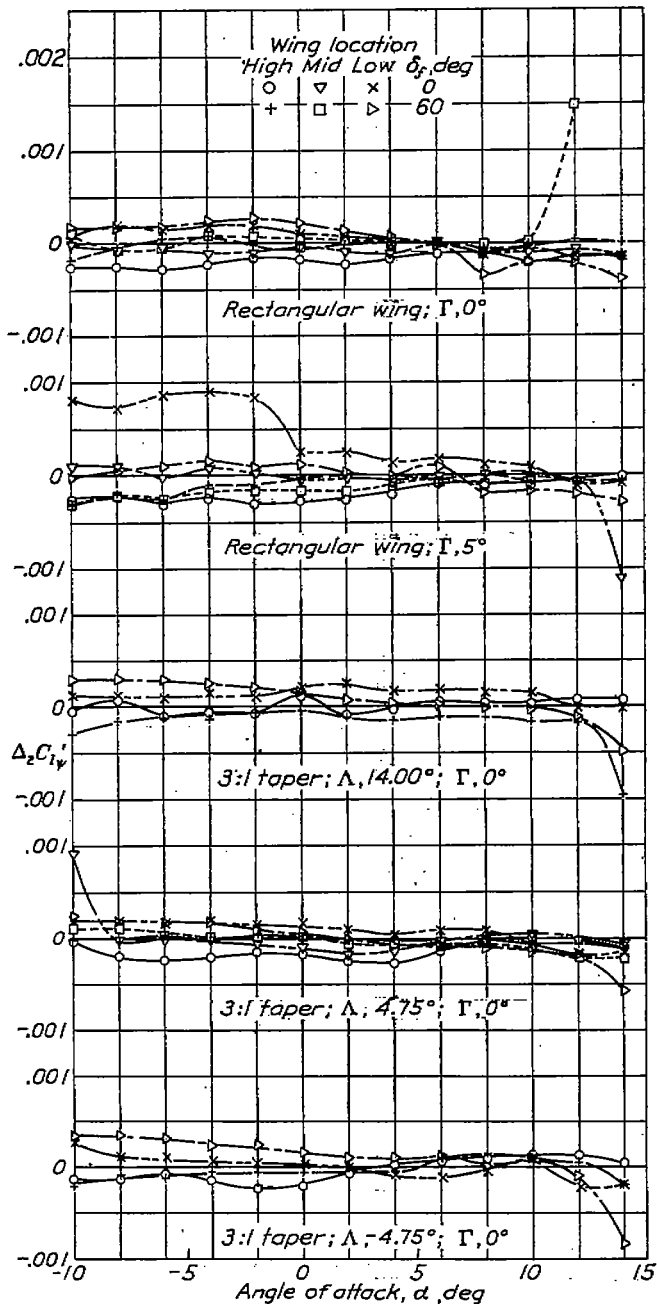
FIGURE 18.—Concluded.



(b) Elliptical fuselage.

FIGURE 19.—Effect of wing-fuselage interference on  $C_{Y'_{\psi}}$  due to fin. NACA 23012 wings.

causes a decrease in  $C_{Y'_{\psi}}$ . Increasing the sweepback increases the effect of  $C_L$  on  $C_{i'_{\psi}}$ . It should be noted that, for the tapered wing with the leading edge straight ( $\Lambda = -4.75^\circ$ ),  $C_{i'_{\psi}}$  decreases with an increase in  $C_L$  while, for the other wings,  $C_{i'_{\psi}}$  increases with increase in  $C_L$ . The most important effect of deflecting the flaps is algebraically to decrease  $C_{x'_{\psi}}$  and  $C_{Y'_{\psi}}$ ; decreasing  $C_{x'_{\psi}}$  increases the stable yawing moment of the wings.



(a) Circular fuselage. (Data for rectangular wing was obtained from reference 5.)  
 FIGURE 19.—Effect of wing-fuselage interference on  $C_l'_{\psi}$  due to fin. NACA 23012 wings.

WING AND FUSELAGE

Increment of  $C_l'_{\psi}$  caused by wing-fuselage interference.—Values of  $\Delta_1 C_l'_{\psi}$  equivalent to an increase in dihedral from  $2^\circ$  to  $6^\circ$  were obtained with the wing in the high position; with the wing in the low position, the effective dihedral was decreased from  $2^\circ$  to  $5^\circ$ . The change in effective dihedral with the wing in the mid-position was  $1^\circ$  or less. (See fig. 14.) These results are in agreement with the theory previously given.

The reversal of the curves of  $\Delta_1 C_l'_{\psi}$  for the low-wing monoplane is of interest. The values of  $\Delta_1 C_l'_{\psi}$  are negative for the range of low angles of attack but, as the

angle of attack is increased, the curves change slope sharply and become positive. This characteristic can be explained by the interference burble mentioned in reference 8. The interference burble is evidenced by a premature stalling of the portion of the wing near the fuselage. When the model is yawed, the interference burble appears first on the down-wind side of the fuselage because of the large pressure gradient. As the stall spreads, the value of  $\Delta_1 C_l'_{\psi}$ , which originally was negative, becomes smaller and then changes sign. The angle of attack at which the interference burble occurs is the angle at which the change in slope of the curve of  $\Delta_1 C_l'_{\psi}$  becomes apparent.

The data given in figures 4 to 6 were compared with the data of reference 3 for wings alone (figs. 11 to 13) to find the angle at which the interference burble occurred. These angles checked in every case with the angles found in figure 14. The angle at which the interference burble occurs is probably dependent on the scale of the tests.

Reference 8 shows that the interference burble caused by a poor wing-fuselage juncture on a low-wing monoplane may be eliminated by filleting. It may therefore be inferred that the irregularities in the lateral-stability characteristics induced by the interference burble may be delayed by the use of suitable fillets; no fillets were used on the present models.

Of the other variables, fuselage shape for a given cross-sectional area appeared to have an appreciable effect on the value of  $\Delta_1 C_l'_{\psi}$ , much larger values being obtained with the elliptical than with the circular fuselage (fig. 14). Inasmuch as the yawed elliptical fuselage develops more lateral force than the yawed circular fuselage, the larger values of  $\Delta_1 C_l'_{\psi}$  obtained with the elliptical fuselage are consistent with the theory of the change in span loading.

The effects of wing taper and of longitudinal position of the wing on the fuselage are interdependent because each of the wings was tested at a different longitudinal position in order to locate the mean aerodynamic center of the wing at the assumed center of gravity of the model for all combinations. In general, the absolute values of  $\Delta_1 C_l'_{\psi}$  increased as the sweep was increased. This change is believed to be largely

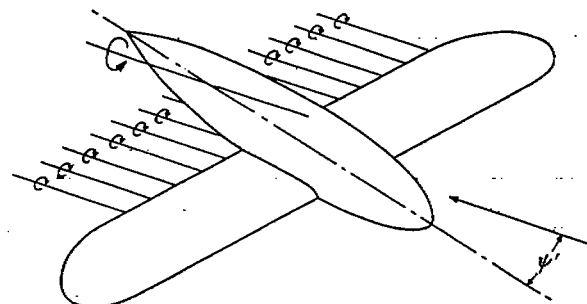


FIGURE 20.—Vortex field caused by interference for the low-wing monoplane.

caused by the change in longitudinal position of the wing rather than by the change in sweep since the wings were moved forward on the fuselage as the sweep was increased. Further tests are planned to determine the separate effects of sweep and longitudinal position. Larger values of  $\Delta_1 C_{l'_{\psi}}$  were obtained with the rectangular wing than with the tapered wing. The rectangular wing was higher on the fuselage than the tapered wings, which might account for part of the increase in  $\Delta_1 C_{l'_{\psi}}$ .

Dihedral appears, in general, to increase the value of  $\Delta_1 C_{l'_{\psi}}$  except for the low-wing monoplane with flaps neutral (fig. 14 (a)).

**Increment of  $C_{Y'_{\psi}}$  caused by wing-fuselage interference.**—The values of  $\Delta_1 C_{Y'_{\psi}}$  are positive for both the high-wing and the low-wing monoplanes; for the mid-wing combination, the values are small. (See fig. 15.) When the high-wing or the low-wing monoplane is yawed, the wing acts as a partial end plate, which tends to increase the lateral force on the fuselage. Larger values of  $\Delta_1 C_{Y'_{\psi}}$  were obtained with the elliptical than with the circular fuselage.

The effect of dihedral on  $\Delta_1 C_{Y'_{\psi}}$  was largely dependent on wing position (fig. 15 (a)). An increase in dihedral was accompanied by a corresponding increase in  $\Delta_1 C_{Y'_{\psi}}$  for the high-wing monoplane; for the low-wing model, the opposite effect was noticed; and, for the midwing model, the effect of dihedral was inconsistent.

Flap deflection acted to increase  $\Delta_1 C_{Y'_{\psi}}$  with the wing in both the mid position and the low position; with the wing in the high position, however, the effect of flap deflection was irregular. No consistent effect of sweep, taper, or plan form appeared.

**Increments of  $C_{n'_{\psi}}$  caused by wing-fuselage interference.**—The values of  $\Delta_1 C_{n'_{\psi}}$  are, in general, stable and of considerable magnitude (fig. 16). For the circular fuselage and the rectangular wing, flaps neutral,  $\Delta_1 C_{n'_{\psi}}$  is from two to three times the value of  $C_{n'_{\psi}}$  for the wing alone and is of sufficient magnitude to balance from 25 to 60 percent of the unstable yawing moment of the fuselage. The maximum value of  $\Delta_1 C_{n'_{\psi}}$  obtained with the tapered wings and the circular fuselage was about half that for the rectangular wing. Slightly larger stable values of  $\Delta_1 C_{n'_{\psi}}$  were obtained with the elliptical fuselage except for the rectangular wing in the midposition. For some cases with flaps deflected the values of  $\Delta_1 C_{n'_{\psi}}$  are large enough to balance the entire unstable yawing moment of the fuselage.

A comparison of the values of  $\Delta_1 C_{n'_{\psi}}$  with those of  $\Delta_1 C_{Y'_{\psi}}$  given in figure 15 indicates that the value of  $\Delta_1 C_{n'_{\psi}}$  is mainly dependent on the change in magnitude and the change in the center of pressure of the lateral

force. As  $\Delta_1 C_{n'_{\psi}}$  is stable and  $\Delta_1 C_{Y'_{\psi}}$  is positive for the high-wing and the low-wing monoplanes, it is apparent that the lateral force back of the assumed center of gravity of the fuselage increases algebraically and that the center of pressure of the fuselage moves back when the wing is added to the fuselage.

The effect of the interference burble is again evident in the results for the low-wing monoplane with the tapered wing having a straight leading edge ( $\Lambda = -4.75^\circ$ ). (See figs. 14 (a) and 16 (a).) With the flaps deflected, the interference burble causes a large loss in lateral force on the fuselage and also a large reduction in unstable yawing moment because of the separation of the flow along the down-wind side of the fuselage. With the flaps neutral, the unstable moment decreases with no loss in lateral force.

Inasmuch as the addition of the wing to the fuselage changes the load distribution along the fuselage, the longitudinal position of the wing on the fuselage appears to be an important factor in the load distribution.

#### WING, FUSELAGE, AND FIN

**Effect of wing-fuselage interference on tail effectiveness.**—The position of the wing on the fuselage has an important bearing on the effectiveness of the vertical tail surfaces. The values of  $\Delta_2 C_{Y'_{\psi}}$ , flaps neutral, are about 0.002 or less for the low-wing monoplane,  $\pm 0.001$  for the midwing combination, and  $-0.003$  or less for the high-wing model (fig. 17). Comparing these values with those for the fuselage and the fin (fig. 10) shows that changing the position of the wing on the fuselage may change the lateral force on the fin as much as  $\pm 40$  percent.

The changes in  $\Delta_2 C_{Y'_{\psi}}$  shown by the results are believed to be largely caused by a change in effective angle of attack of the fin; such a conclusion is in agreement with the explanation previously given. (See fig. 20.)

The values of  $\Delta_2 C_{Y'_{\psi}}$  are algebraically increased as much as 0.002 by flap deflection. Flap deflection therefore appears to be about as important as the position of the wing on the fuselage in determining the magnitude of the wing-fuselage interference on the vertical fin.

The effect of dihedral is small and acts to decrease  $\Delta_2 C_{Y'_{\psi}}$  algebraically (fig. 17 (a)). A possible explanation of this characteristic is a change in the vortex field and a consequent change in the lateral flow at the tail. When a wing having dihedral is yawed, an unsymmetrical span load distribution results. The vortices shed near the center of the wing, because of the change in slope of the load-distribution curve, rotate in such a manner as to reduce the effective angle of attack of the fin as a result of the induced lateral flow.

The values of  $\Delta_2 C_{Y'}_{\psi}$  obtained with the elliptical fuselage (fig. 17 (b)) increase with increase in angle of attack, which is not the case with the circular fuselage (fig. 17 (a)). As previously mentioned, the effectiveness of the fin on the elliptical fuselage decreased with increase in angle of attack because of a partial blanketing of the fin by the fuselage (fig. 10). Apparently, wing-fuselage interference tends to reduce this blanketing.

The variations in  $\Delta_2 C_{Y'}_{\psi}$  are, for the most part, reflected in the values of  $\Delta_2 C_{n'}_{\psi}$  (fig. 18). The interference acts to increase the stable moment produced by the fin of the low-wing monoplane and values of  $\Delta_2 C_{n'}_{\psi}$  of  $-0.0013$  or less are obtained. For the high-wing monoplane, the values of  $\Delta_2 C_{n'}_{\psi}$  are unstable; the maximum value is about  $0.0010$ . The values of  $\Delta_2 C_{n'}_{\psi}$  are small for the midwing monoplane with both the circular and the elliptical fuselage at zero angle of attack. With the elliptical fuselage (fig. 18(b)), the values of  $\Delta_2 C_{n'}_{\psi}$  vary with angle of attack as did the values of  $\Delta_2 C_{Y'}_{\psi}$ , the model becoming more stable as the angle of attack is increased.

Flap deflection is strongly stabilizing, but dihedral tends to reduce stability in yaw.

Effect of interference on the rolling moment produced by the fin.—The effect of interference on the rolling moment produced by the fin is small (fig. 19). Values of  $\Delta_2 C_{l'}_{\psi}$  obtained were equivalent to a  $\pm 1^\circ$  change in effective dihedral; in general, the effective dihedral was increased with the wing in the low position and decreased with the wing in the high position.

#### CONCLUDING REMARKS

It should be remembered that the model was tested without a horizontal tail and that the horizontal tail probably exerts an appreciable effect on the efficiency of the vertical tail.

The results showed that wing position had a pronounced effect on lateral-stability characteristics. Wing-fuselage interference increased the effective dihedral in the order of  $5^\circ$  for the high-wing monoplane, and a corresponding decrease in effective dihedral was obtained for the low-wing combination. With flaps neutral the maximum effect of wing-fuselage interference was of sufficient magnitude to balance 60 percent of the unstable yawing moment of the fuselage; with flaps deflected the magnitude of the interference effect was sufficient to balance the entire unstable yawing moment of the fuselage.

The lateral force on the fuselage was increased when a wing was placed in the high or the low position.

Fin effectiveness was influenced by the change in the vortex field caused by wing-fuselage interference. The fin effectiveness of the high-wing monoplane was de-

creased as much as 40 percent and that of a low-wing monoplane was increased a maximum of 80 percent. Flap deflection increased the fin effectiveness as much as 50 percent. Dihedral, in general, decreased the fin effectiveness.

LANGLEY MEMORIAL AERONAUTICAL LABORATORY,  
NATIONAL ADVISORY COMMITTEE FOR AERONAUTICS,  
LANGLEY FIELD, VA., August 8, 1940.

#### REFERENCES

- Zimmerman, Charles H.: An Analysis of Lateral Stability in Power-Off Flight with Charts for Use in Design. Rep. No. 589, NACA, 1937.
- Shortal, Joseph A.: Effect of Tip Shape and Dihedral on Lateral-Stability Characteristics. Rep. No. 548, NACA, 1935.
- Bamber, M. J., and House, R. O.: Wind-Tunnel Investigation of Effect of Yaw on Lateral-Stability Characteristics. I—Four N. A. C. A. 23012 Wings of Various Plan Forms with and without Dihedral. T. N. No. 703, NACA, 1939.
- Pearson, Henry A., and Jones, Robert T.: Theoretical Stability and Control Characteristics of Wings with Various Amounts of Taper and Twist. Rep. No. 635, NACA, 1938.
- Bamber, M. J., and House, R. O.: Wind-Tunnel Investigation of Effect of Yaw on Lateral-Stability Characteristics. II—Rectangular N. A. C. A. 23012 Wing with a Circular Fuselage and a Fin. T. N. No. 730, NACA, 1939.
- Wenzinger, Carl J., and Harris, Thomas A.: Wind-Tunnel Investigation of an N. A. C. A. 23012 Airfoil with Various Arrangements of Slotted Flaps. Rep. No. 664, NACA, 1939.
- Harris, Thomas A.: The 7 by 10 Foot Wind Tunnel of the National Advisory Committee for Aeronautics. Rep. No. 412, NACA, 1931.
- Jacobs, Eastman N., and Ward, Kenneth E.: Interference of Wing and Fuselage from Tests of 209 Combinations in the N. A. C. A. Variable-Density Tunnel. Rep. No. 540, NACA, 1935.
- Zimmerman, C. H.: Characteristics of Clark Y Airfoils of Small Aspect Ratios. Rep. No. 431, NACA, 1932.

TABLE I  
DIMENSIONS OF FUSELAGES  
[All dimensions in in.]

Station	Circular	Elliptical	
	Diameter	Major axis	Minor axis
0	0	0	0
.312	1.544	2.044	1.168
.812	2.484	3.288	1.878
1.312	3.144	4.168	2.376
2.812	4.088	5.408	3.090
4.312	5.300	7.010	4.006
8.312	6.476	8.564	4.804
12.312	6.820	9.020	5.154
16.312	6.880	9.100	5.200
20.312	6.812	9.010	5.148
24.312	6.536	8.646	4.940
28.312	5.980	7.910	4.620
32.312	5.032	6.658	3.804
34.312	4.340	5.740	3.280
36.312	3.396	4.404	2.568
38.312	2.000	2.646	1.612
39.312	1.096	1.460	.828
40.312	0	0	0